THE JOURNAL OF BIOLOGICAL CHEMISTRY VOL. 288, NO. 25, pp. 18146–18161, June 21, 2013

Lacritin Rescues Stressed Epithelia via Rapid Forkhead Box O3 (FOXO3)-associated Autophagy That Restores Metabolism*[S]

Received for publication, November 14, 2012, and in revised form, May 1, 2013 Published, JBC Papers in Press, May 2, 2013, DOI 10.1074/jbc.M112.436584

Ningning Wang[‡], Keith Zimmerman[‡], Ronald W. Raab[§], Robert L. McKown[§], Cindy M. L. Hutnik[¶], Venu Talla[‡], Milton F. Tyler, IV[‡], Jae K. Lee[‖], and Gordon W. Laurie[‡ ‡‡1]**

*From the Departments of [‡]Cell Biology, [‖]Public Health Sciences, **Systems and Information Engineering, and [‡‡]Ophthalmology, University of Virginia, Charlottesville, Virginia 22908, [§]Department of Integrated Science and Technology, James Madison University, Harrisonburg, Virginia 22807, and [¶]Department of Ophthalmology, University of Western Ontario, London, Ontario N6A 4V2, Canada*

Background: Homeostatic regulation of epithelia influences disease acquisition and aging.
Results: Prosecretory mitogen lacritin stimulates FOXO3-ATG101 and FOXO1-ATG7 autophagic coupling and restores metabolic homeostasis.
Conclusion: Lacritin is a homeostatic regulator.
Significance: Exogenous lacritin restores prohomeostatic activity to tears from dry eye individuals.

Homeostasis is essential for cell survival. However, homeostatic regulation of surface epithelia is poorly understood. The eye surface, lacking the cornified barrier of skin, provides an excellent model. Tears cover the surface of the eye and are deficient in dry eye, the most common eye disease affecting at least 5% of the world's population. Only a tiny fraction of the tear proteome appears to be affected, including lacritin, an epithelium-selective mitogen that promotes basal tearing when topically applied to rabbit eyes. Here we show that homeostasis of cultured corneal epithelia is entirely lacritin-dependent and elucidate the mechanism as a rapid autophagic flux to promptly restore cellular metabolism and mitochondrial fusion in keeping with the short residence time of lacritin on the eye. Accelerated flux appears to be derived from lacritin-stimulated acetylation of FOXO3 as a novel ligand for ATG101 and coupling of stress-acetylated FOXO1 with ATG7 (which remains uncoupled without lacritin) and be sufficient to selectively divert huntingtin mutant Htt103Q aggregates largely without affecting non-aggregated Htt25Q. This is in keeping with stress as a prerequisite for lacritin-stimulated autophagy. Lacritin targets the cell surface proteoglycan syndecan-1 via its C-terminal amino acids Leu[108]-Leu[109]-Phe[112] and is also available in saliva, plasma, and lung lavage. Thus, lacritin may promote epithelial homeostasis widely.

Homeostasis is an essential and dynamic property of all unicellular and multicellular organisms (1) with overlapping positive and negative feedback loops (2) that sense and continually adjust to environmental and intrinsic changes. Inadequate control can trigger developmental abnormalities, disease, or death (3). How homeostasis is controlled is an investigative area with wide biological significance.

Macroautophagy (hereafter referred to as autophagy) contributes to the regulation of homeostasis. Autophagy is a stimulatable self-catabolic pathway that constitutively clears damaged proteins and organelles (2) and displays cross-talk with the proteasome (4) together in a manner thought to involve the FOXO[2] family members FOXO1 and FOXO3. FOXO1 becomes acetylated in stress. Acetylated FOXO1 captures ATG7 to trigger autophagy (5). FOXO3 augments transcription of autophagic mediators ULK1, AMP-activated protein kinase, and MAPLC3B (LC3) to enhance autophagic responsiveness of metabolically stressed hemopoietic stems cells (6), although FOXO3 is better known as a transcription factor for cell death (7). How FOXO1 and FOXO3 precisely modulate autophagy to regulate homeostasis is not clear. Harnessing such mechanisms may have wide benefit in neurodegenerative, tumorigenic, autoimmune, and infectious diseases (8).

Stress is sudden and varied on surface epithelia, particularly on the eye where the cornified barrier protecting skin is replaced by tears, the ~3-μm-thick fluid comprising metabolites (9), lipids (10), and in a recent estimate over 1500 different proteins (11). Homeostatic dysregulation of the surface of the

* This work was supported, in whole or in part, by National Institutes of Health Grants RO1 EY013143 and EY018222 (to G. W. L.).
[S] This article contains supplemental Fig. 1 and Tables 1 and 2.
[1] To whom correspondence should be addressed: Depts. of Cell Biology and Ophthalmology, University of Virginia, 1340 Jefferson Park Ave., Charlottesville, VA 22908. Tel.: 434-924-5250; Fax: 434-982-3912; E-mail: glaurie@virginia.edu.

[2] The abbreviations used are: FOXO, forkhead box O; ATG, autophagy-related; IFNG, interferon-γ; ULK1, unc-51-like kinase 1; p62, SQSTM1 (sequestrome 1); Alfy, WDFY3 (WD repeat and FYVE domain-containing 3); LC3, MAP1LC3B (microtubule-associated protein 1 light chain 3β); LC3/RG, HCE-T cells stably expressing pBABE-puro mCherry-EGFP-LC3B; MTT, 3-(4,5-dimethyl-2-yl)-2,5-diphenyltetrazolium bromide); FCCP, carbonyl cyanide 4-(trifluoromethoxy)phenylhydrazone; xyloside, 4-methylumbelliferyl-β-D-xylopyranoside; S6K, RPS6KB1 (ribosomal protein S6 kinase, 70 kDa, polypeptide 1); TRAF6, TNF receptor-associated factor 6 (E3 ubiquitin protein ligase); mTOR, mechanistic target of rapamycin (serine/threonine kinase); HCE-T, human corneal epithelial; Htt, huntingtin; MEM, minimum essential medium; EGFP, enhanced GFP; mCFP, monomeric cyan fluorescent protein; ANOVA, analysis of variance; UGT, UDP-glucuronyltransferase; FOXO3Nt, dominant negative FOXO3.

eye in "dry eye," a tear insufficiency syndrome(s) and the most common eye disease (12), offers some potential etiological clues because surprisingly few tear proteins show any disease-associated change. The only known growth factor-like molecule affected is lacritin (13–16), a ~25-kDa prosecretory mitogen (17) also detected in saliva (18), plasma (19), and lung lavage (Human Proteinpedia HuPA_00022). Lacritin displays partial homology with dermcidin (20). The Y-P30 peptide of dermcidin promotes neuronal survival by a mechanism involving the heparan sulfate-dependent nucleation of syndecan-2 or -3 with pleiotrophin, a neuritogenic cytokine (21).

We now report that low nanomolar lacritin restores homeostasis to corneal epithelial cells stressed with the inflammatory cytokines interferon-γ (IFNG) and tumor necrosis factor (TNF), both sources of stress in dry eye. Lacritin appears to do so by promoting rapid FOXO3 acetylation and coupling of FOXO3 with ATG101. ATG101 is an autophagic mediator known to bind and stabilize the ATG13-ULK1 complex responsible for initiating autophagy (22, 23). Furthermore, lacritin treatment is a prerequisite for stress-acetylated FOXO1-ATG7 coupling. Lacritin targets cells via its C-terminal hydrophobic Leu^{108}-Leu^{109}-Phe^{112} domain, which is known to bind GAGAL in the N terminus of syndecan-1 (24) through a heparanase off-on switch (25). Tears immunodepleted of lacritin or dry eye tears fail to restore homeostasis. However, spiking lacritin into dry eye tears restored homeostasis. Thus, lacritin is a prosurvival factor, potentially available to many epithelia, that stimulates autophagy to restore homeostasis and may serve as a master protector of the eye.

EXPERIMENTAL PROCEDURES

Cell Culture, Constructs, and Antibodies—Human corneal epithelial (HCE-T) cells were purchased from the RIKEN BioResource Center (Tsukuba-shi, Japan) and used between passages 3 and 15. HCE-T cells were cultured and maintained in DMEM/F-12 containing 4 mg/ml insulin, 100 μg/ml EGF, 500 μg/ml cholera toxin, and 5 μl/ml DMSO. Primary human corneal epithelial cells (PCS-700-010) were purchased from ATCC (Manassas, VA) and expanded in the suggested medium.

N-terminal deletions of 45, 65, and 71 amino acids and point mutants V69S, I73S, I98S, F104S, L108S, L109S, F112S, I68S/I73S, V91S/L109S, and L108S/L109S/F112S were developed from pLAC (26) using the primers indicated in supplemental Table 1. All constructs were confirmed by DNA sequencing. Lacritin and deletion or point mutants, including deletion mutant "C-25" (26), were generated in *Escherichia coli* and purified as described previously (26) with additional purification over DEAE in PBS in which lacritin is collected in the flow-through. Purified lacritin was filter-sterilized and stored lyophilized.

Polyclonal N and C terminus-specific anti-lacritin antibodies were respectively generated in New Zealand White rabbits against keyhole limpet hemocyanin-conjugated EDASSDSTGADPAQEAGTS ("Pep Lac N-Term") as "anti-Pep Lac N-term" (27) and against lacritin deletion mutant N-65 as "anti-N-65 Lac C-term" (Bio-Synthesis Inc., Lewisville, TX) and characterized. Monoclonal N terminus-specific anti-lacritin antibodies were generated (University of Virginia Lymphocyte Culture Center) in mice against keyhole limpet hemocyanin-conjugated DPAQEAGTSKPNEEIS and screened through three rounds of cloning against the lacritin deletion mutant C-59 as 1F5-C9-F4 ("1F5"; IgG1).

Subcloning and shRNAs—HCE-T cells were transduced in Opti-MEM (Invitrogen) followed by puromycin or hygromycin selection in DMEM/F-12. Transduction was carried out with lentiviral particles encoding shRNAs directed to ATG7, FOXO3, and ATG101 or with empty vector or non-targeting control (Dharmacon, Waltham, MA), and transduced cells were stably selected.

For autophagy flux studies, HCE-T cells were transduced in Opti-MEM with retroviral particles encoding pBABE-puro mCherry-EGFP-LC3B and stably selected as "LC3/RG" cells. pBABE-puro mCherry-EGFP-LC3B was purchased from Addgene (plasmid 22418; originally developed in pDest (28)). Other LC3/RG cells were transiently transduced with pBABE-hygro Htt25Q-mCFP or pBABE-hygro Htt103Q-mCFP particles. pcDNA Htt25Q-mCFP and Htt103Q-mCFP (29) were kindly provided by Ai Yamamoto (Columbia University) and subcloned into pBABE-hygro (Addgene plasmid 1765). Recombinant retroviral particles were generated using the Platinum Retrovirus Expression System, Pantropic (Cell Biolabs, San Diego, CA).

Tears and Viability Analyses—Tears were collected from 0.5% proparacaine-anesthetized eyes from a total of 48 normal or dry eye individuals (supplemental Table 2) by insertion of a filter wicking "Schirmer" strip with millimeter gradations between the lid and eye and individually stored at −70 °C. Human procedures and patient consent were approved by the University of Western Ontario and University of Virginia Institutional Review Boards. Prior to elution, the total normal or dry eye tear volume was estimated from millimeters of tears drawn into each strip. This defined the final volume of PBS respectively used for elution. Pooled normal or pooled dry eye tears were stored at −70 °C until use.

For FOXO3 translocation assays, HCE-T cells were grown in triplicate to subconfluence (~50%) on coverslips in α-MEM (5.54 mM glucose), sensitized overnight in IFNG (100 units/ml; Roche Applied Science), and treated for 15 min with normal or dry eye tears diluted 1:100 in α-MEM together with TNF (50 ng/ml; PeproTech, Rocky Hill, NJ) without or with 10 nM lacritin or C-25. Cells were washed, fixed with 4% paraformaldehyde, and immunostained for FOXO3 (1:200; Millipore, Billerica, MA) followed by goat anti-rabbit secondary antibody and visualization on a Zeiss LSM 700 microscope.

Some experiments were performed with normal tears that had been immunodepleted of lacritin. For immunodepletion, rabbit anti-Pep Lac N-term and anti-N-65 Lac C-term were jointly immobilized on protein A beads and washed. A rabbit preimmune column was similarly prepared for mock-depleted tears. The flow-through from overnight incubation of each with normal tears was collected and assayed in triplicate on IFNG-sensitized cells with TNF as described above. For validation, the acid eluant from each column was separated by SDS-PAGE, transferred to nitrocellulose, and blotted for lacritin using mouse anti-lacritin antibody 1F5 and a mouse-specific, perox-

idase-labeled secondary antibody followed by chemiluminescence detection.

Viability was monitored using the 3-(4,5-dimethyl-2-yl)-2,5-diphenyltetrazolium bromide) (MTT) reduction assay (Invitrogen) or a Nucleocounter (New Brunswick Scientific, Edison, NJ). Cells were seeded overnight in 24-well plates at a density of 500 cells/mm^2 to give rise to ~80% confluence the next day. Then cells were sensitized overnight in IFNG (100 units/ml) in α-MEM and treated in triplicate for 15 min with 10 nM lacritin or lacritin deletion or point mutants or with different lacritin doses in α-MEM together with TNF as described above.

Inclusion of inhibitors was simultaneous with the addition of lacritin or C-25 in all viability and other experiments except where otherwise noted. Inhibitors included PI103 (0.5 μM; EMD, Darmstadt, Germany), rapamycin (10 and 100 nM; EMD), and cyclosporin A (0.1 μM; EMD). One exception was 4-methylumbelliferyl-β-D-xylopyranoside ("xyloside"; 70 and 80 nM; Sigma), which was added during IFNG sensitization and during treatment with TNF and lacritin. The assay was completed by addition of MTT (5 mg/ml) to each well (at 37 °C for 4 h) followed by isopropanol with 0.04 N HCl and measurement at 570 nm using a reference wavelength of 630 nm. Viability was assayed in a Nucleocounter (New Brunswick Scientific).

LC3 Blotting and Autophagic Flux—IFNG/TNF-stressed cells in 24-well plates treated exactly as above without or with lacritin or C-25 for different times and with or without inhibitors were extracted with radioimmune precipitation assay buffer (Millipore) containing 1% SDS and protease inhibitors. Lysates were separated by 12% SDS-PAGE, transferred to nitrocellulose, and blotted for LC3B (MBL International, Woburn, MA). IFNG/TNF- or IFNG/TNF plus lacritin-induced autophagic flux was analyzed by inclusion of leupeptin (0.1 and 1 μM; EMD), vinblastine (0.05 and 0.5 μM; EMD), and wortmannin (0.1 and 1 μM; EMD).

To visually monitor autophagic flux, LC3/RG (pBABE-puro mCherry-EGFP-LC3B) cells were grown in triplicate on coverslips and stressed as above with IFNG/TNF with 10 nM lacritin or C-25 without or with vinblastine (0.05 μM). Cells were monitored over time for EGFP and mCherry spectra using a Zeiss LSM 700 confocal microscope. Protein aggregation in LC3/RG/Htt25Q or /Htt103Q cells was monitored by jointly following the mCFP spectrum. For analysis of apoptosis, radioimmune precipitation assay (1% SDS) lysates of IFNG/TNF-stressed cells without or with lacritin (as described above) or cells that were not stressed were blotted for caspase 9 or 3 (both from Cell Signaling Technology).

Immunoprecipitation and Blotting—Radioimmune precipitation assay (1% SDS) lysates from cells stressed as described above in the absence or presence of lacritin or C-25 for different times and at different doses were subjected to FOXO1 or FOXO3 immunoprecipitation and then blotted for acetyl-lysine (Abcam, Cambridge, MA) or ATG7 (MBL International). FOXO3 immunoprecipitates were also blotted for ATG3, ATG4B, ATG12, ATG101, LC3B, p62 (MBL International), or ubiquitin (Bethyl Laboratories, Montgomery, TX). LC3 immunoprecipitates were similarly collected and blotted for p62 (MBL International), Alfy, and ubiquitin (Bethyl Laboratories).

Metabolic Analyses—Cells plated (10.9 cells/mm^2) in replicates of 10 in wells of Seahorse 24-well plates (Seahorse Bioscience, North Billerica, MA) were stressed with IFNG as above, treated with lacritin or C-25 (10 nM) with TNF, and then immediately monitored in an XF24 Analyzer (Seahorse). The oxygen consumption rate was measured without or after sequential addition of oligomycin (500 nM), carbonyl cyanide 4-(trifluoromethoxy)phenylhydrazone (FCCP; 375 nM), rotenone (1 μM), and antimycin (750 nM) after washing. After treatment with each inhibitor, cells were mixed, rested, and then read three times. Inhibitors were purchased from Seahorse as part of the XF Cell Mito Stress kit.

Mitochondrial dynamics were monitored after MitoTracker Red FM (Invitrogen) staining. Briefly, live IFNG-sensitized normal or shATG7 knockdown cells on coverslips were stained for 30 min with 50 nM MitoTracker Red FM in Dulbecco's PBS, rinsed two times with Dulbecco's PBS, and reimmersed in α-MEM to which TNF was added in the presence of lacritin or C-25 (10 nM). Live mitochondria were then monitored at 20-s intervals for 30 min on a PerkinElmer UltraVIEW VoX spinning disc confocal microscope with a seven-slice Z-stack. Fission frequency was estimated from the ComponentCount feature of Mytoe. The number of individual pieces of the mitochondrial skeleton was counted at each frame, and from this, the number of fission or fusion events per second was determined where an increase in number indicated a fission event and a decrease indicated a fusion event.

For metabolomic analysis, cells stressed as above were treated in replicates of six with TNF and lacritin or C-25 (10 nM) or without lacritin or C-25 ("untreated") for 10 min at ~10^6 cells/sample, then gently scraped, spun, and washed in PBS, and the pellet was snap frozen. Metabolite analysis was performed in an unbiased manner by Metabolon (Durham, NC) using liquid and gas chromatography coupled to mass spectrometry. Instrument (internal standards) and total process (endogenous biochemicals) variability was 4 and 11%, respectively. 135 metabolites were identified.

Statistical Analyses—All experiments (with the exception of the single metabolomic analysis) were performed at least three times. Prior to statistical analysis, raw metabolite data values were log-transformed to make their highly skewed data distribution closer to a Gaussian distribution for satisfying statistical analysis assumptions. Statistical significance of differentially activated metabolites was assessed both by two-sample *t* test and non-parametric Wilcoxon test of the log-transformed normalized data. Metabolites with both tests were then conservatively considered statistically significant ($p < 0.05$) and further analyzed by a hierarchical clustering method. All other data were analyzed by one-way analysis of variance (ANOVA) with Dunnett's post-test or where appropriate by two-way ANOVA or by the paired two-tailed *t* test. Data are reported as the mean ± S.E.

RESULTS

Tears and Lacritin Restore Homeostasis—To gain insight into epithelial homeostasis, we asked whether tears from normal individuals are cytoprotective (Fig. 1*A*), whether cytoprotection is absent in dry eye tears (Fig. 1*B*), and whether the two can

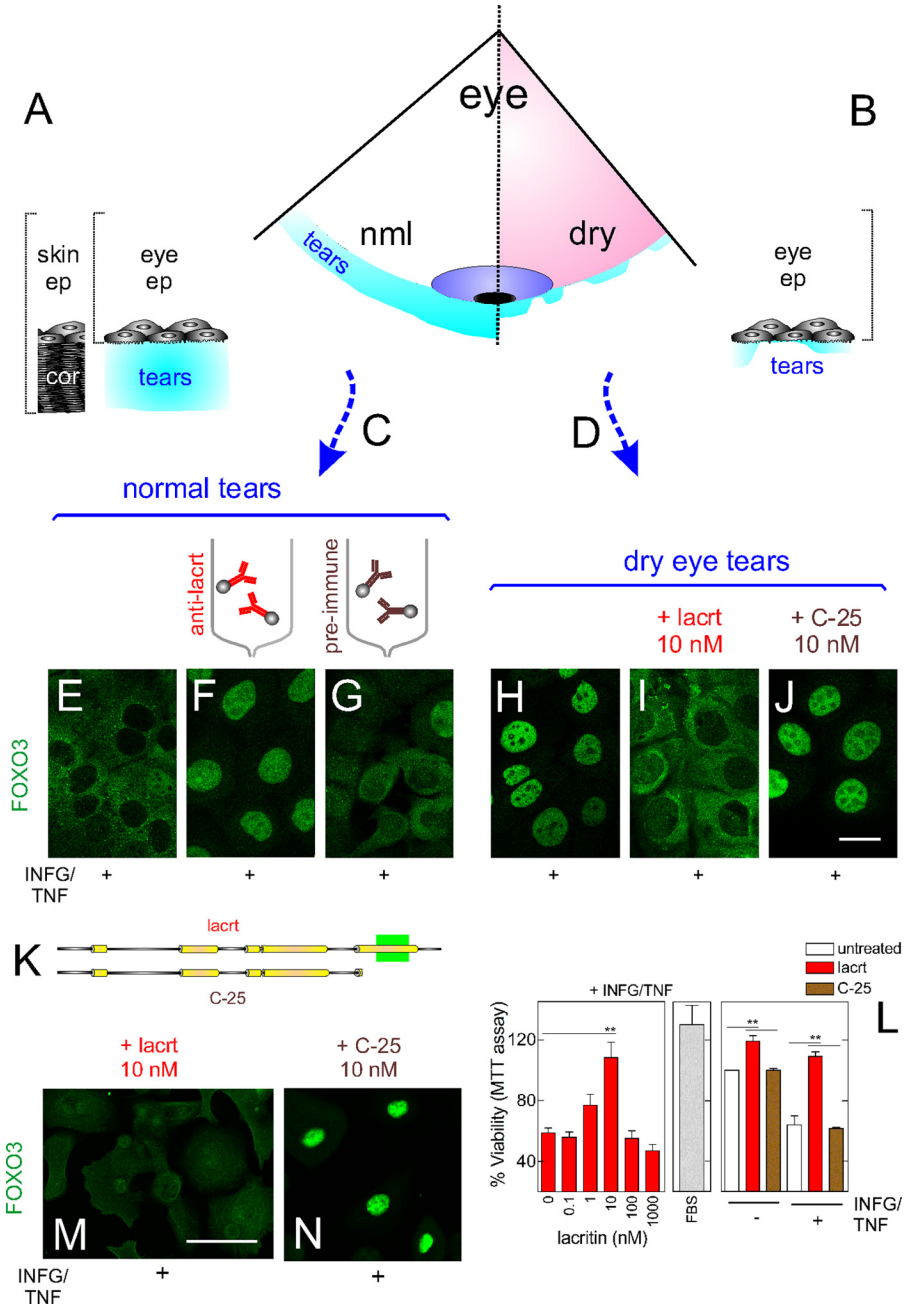

FIGURE 1. **Lacritin in normal human tears is essential for survival of stressed corneal epithelial cells.** *A*, schematic diagram of normal tears on the eye surface as compared with skin with the protective cornified zone. *B*, schematic diagram of tears on the eye in dry eye. *C*, pool of basal human tears from 19 individuals. *D*, pool of dry eye human tears from 29 individuals. *E*, HCE-T cells were sensitized overnight with IFNG and then treated for 15 min with pooled normal tears in the presence of TNF. Cells were washed and fixed, and then FOXO3 was immunolocalized. The same approach with different tear or lacritin samples was used in *F–J* , *M*, and *N*. IFNG/TNF-stressed cells with lacritin-depleted tears (*F*), mock-depleted tears (*G*), pooled dry eye tears (*H*), dry eye tears spiked with 10 nM lacritin (*I*), and dry eye tears spiked with 10 nM C-25 (lacritin lacking 25 amino acids from the C terminus) (*J*). *Bar*, 10 μm. *K*, linear diagram of lacritin *versus* C-25. *Yellow* indicates demonstrated (15) and predicted α-helices. *L*, *left panel*, HCE-T cells were sensitized overnight with IFNG and then treated for 15 min with increasing amounts of lacritin (or FBS (*middle panel*)) in the presence of TNF. Viability was assessed by the MTT assay. 10 nM lacritin, but not other doses, significantly enhanced cell viability (ANOVA with Dunnett's post-test; **, $p < 0.01$) but is not significantly different from FBS-enhanced viability ($p > 0.05$). *Right panel*, HCE-T cells were similarly stressed with IFNG and TNF or not stressed and then left untreated or instead treated with 10 nM lacritin or C-25. Lacritin enhanced viability (ANOVA with Dunnett's post-test; **, $p < 0.01$). The *y axis* is not shown extending to zero in this and other viability assays because the assay detects subtle changes. *M*, lacritin (10 nM) on IFNG/TNF-stressed primary human corneal epithelial cells. *Bar*, 25 μm. *N*, C-25 (10 nM) on IFNG/TNF-stressed primary human corneal epithelial cells. *Error bars* represent S.E. *cor*, cornified; *lacrt*, lacritin; *ep*, epithelia; *nml*, normal.

be manipulated to identify the activity. Basal tears (supplemental Table 2) from normal individuals (Fig. 1*C*) and from those diagnosed with dry eye (Fig. 1*D*) were incubated with HCE-T cells stressed with the inflammatory cytokines IFNG and TNF, much like their *in vivo* dry eye counterparts (30). Nuclear-cytoplasmic translocation of the corneal transcription factor FOXO3 (7) served as a simple readout for cellular stress with cytoplasmic FOXO3 indicative of restored homeostasis. Nuclear FOXO3 largely transcribes for cell stress or death (7). In stressed cells treated with normal tears, FOXO3 translocated

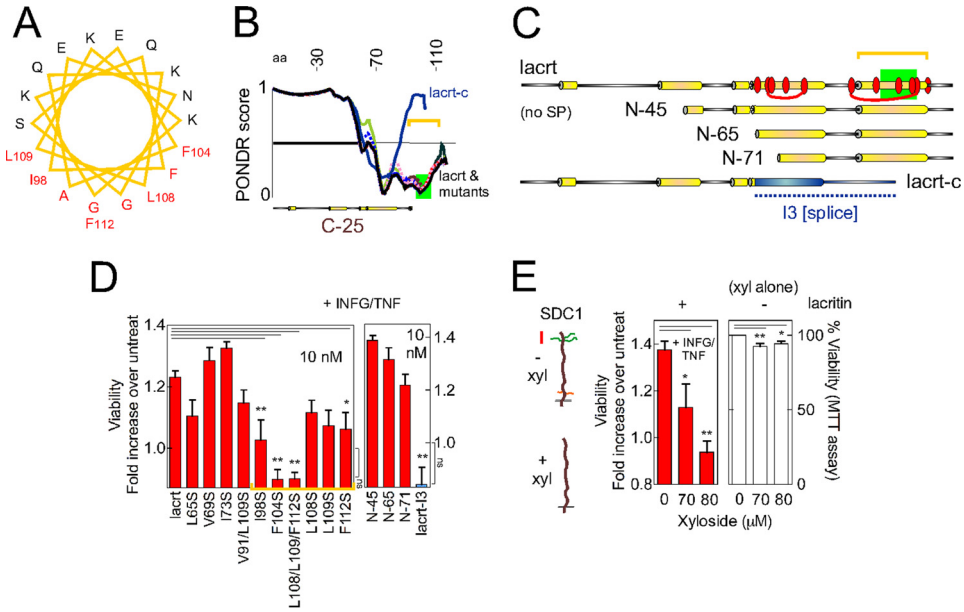

FIGURE 2. **Lacritin survival activity is defined by C-terminal hydrophobic residues Ile^{98}, Phe^{104}, Leu^{108}, Leu^{109}, and Phe^{112}.** *A*, pepwheel analysis of the C-terminal α-helix (amino acids 94–112) of lacritin. *Red* residues are hydrophobic. *B*, Predictor of Naturally Disordered Regions (*PONDR*) tracings of lacritin, lacritin mutants, and splice variant lacritin-c. *0* represents "order," and *1* represents "disorder" with tracing below the *horizontal line* predicted to be ordered. The *green rectangle* approximates the syndecan-1 binding region (17) for cell targeting. *C*, linear diagrams comparing lacritin point (*red ovals*) and truncation mutants and splice variant with the novel I3 C terminus (*blue*). Numbering here and elsewhere excludes the signal peptide. *D*, HCE-T cells were sensitized overnight with IFNG and then treated for 15 min with different lacritin constructs (10 nM) in the presence of TNF. Viability was assessed by the MTT assay and is expressed as the -fold increase in viability, defined as the ratio of experimental viability to the control viability. Control viability was derived from cells treated with IFNG/TNF alone. Several mutants and the splice variant are not prosurvival (ANOVA with Dunnett's post-test; **, $p < 0.01$; *, $p < 0.05$). The viability of F104S, L108/L109/F112S, and lacritin I3-treated cells does not significantly differ from that of IFNG/TNF-stressed cells (ANOVA with Dunnett's post-test, *ns*, not significant, $p > 0.05$. *E*, HCE-T cells were sensitized overnight with IFNG in the presence of no or increasing amounts of xyloside (*left panel*). The next day, cells were treated for 15 min with 10 nM lacritin in the presence of TNF and xyloside. Viability was assessed by the MTT assay. Other cells were only treated overnight with no or increasing amounts of xyloside, and viability was assessed by the MTT assay (*right panel*). Xyloside significantly negates lacritin prosurvival activity. It also significantly reduces cell viability in the absence of IFNG/TNF but only slightly (94 ± 1.6 and 93 ± 1.9% *versus* 100% viability, respectively, for 80 and 90 μM xyloside). Xyloside inhibits heparan and chondroitin sulfate chain attachment and can inhibit hyaluronan synthesis. *Left*, diagrams of untreated (*above*) *versus* xyloside-treated (*below*) syndecan-1 with heparan and chondroitin sulfate side chains depicted in *green* and *red*, respectively. Both are attached to a core protein with a short cytoplasmic domain below the *black line*. *Error bars* represent S.E. *lacrt*, lacritin; *SP*, signal peptide; *xyl*, xyloside; *aa*, amino acids; *untreat*, untreated.

to the cytoplasm (Fig. 1*E*). However, with dry eye tears, FOXO3 remained nuclear (Fig. 1*H*). Thus, normal, but not dry eye, tears are capable of restoring homeostasis.

We explored a role for lacritin (Fig. 1*K*) because it is the only growth factor reported to be selectively down-regulated in dry eye tears (13, 14, 16). Stressed HCE-T cells were incubated with increasing amounts of recombinant lacritin (Fig. 1*L*, *left panel*). Viability was monitored using the MTT reduction assay. The HCE-T cell response to lacritin was bell-shaped with an optimum survival dose of 10 nM (Fig. 1*L*, *left panel*) that returned cells to the viability of their unstressed counterparts. In contrast, lacritin truncation mutant C-25, which lacks 25 amino acids from the C terminus, was inactive (Fig. 1*L*, *right panel*) in keeping with the absence of the C-terminal syndecan-1 binding domain (Fig. 1*K*, *green box*) necessary for cell targeting and lacritin signaling (25, 26).

We next immunodepleted lacritin from normal tears with immobilized rabbit anti-N and -C-terminal lacritin antibodies, although normal tears have other growth factors that might compensate. Also dry eye tears were spiked with lacritin. Dry eye tears are both hyperosmolar and inflammatory cytokine-rich (31). In cells treated with mock-depleted tears, FOXO3 was translocated to the cytoplasm (Fig. 1*G*), whereas FOXO3 remained nuclear in cells treated with lacritin-depleted tears (Fig. 1*F*). In cells treated with dry eye tears spiked with lacritin (Fig. 1*I*), but not those spiked with C-25 (Fig. 1*J*), FOXO3 was translocated to the cytoplasm. Lacritin (Fig. 1*M*), but not C-25 (Fig. 1*N*), treatment also resulted in translocation of FOXO3 in IFNG/TNF-stressed primary human corneal epithelial cells (Fig. 1, *M* and *N*). Thus, lacritin in normal tears appears to be responsible for restoring homeostasis.

Lacritin C-terminal Prohomeostatic Domain—To define the lacritin domain necessary for regulation of homeostasis, truncation and point mutants were generated. Inactivity of the C-25 truncation mutant (Fig. 1, *L* and *N*) defined a cytoprotective domain in the C terminus of lacritin (Fig. 1*K*) that was previously shown to be α-helical and likely amphipathic (Fig. 2*A*) (26) and accordingly ordered (Fig. 2*B*).

The hydrophobic face of amphipathic α-helices can mediate high affinity agonist-receptor or -co-receptor interactions (32). To assay this possibility, hydrophobic residues were singly, doubly, or triply mutated (Fig. 2*C*, *red ovals*). Truncations and the C terminus ("I3") of the lacritin-c splice variant (33, 34) (Fig. 2*C*) with a sequence completely different from wild type were generated.

Hydrophobic face mutants I98S, F104S, L108S/L109S/F112S, and F112S were significantly less active (Fig. 2*D*, *left panel*). Activity was unaffected by mutations L65S, I68S/I78S, V69S, and I73S in an adjacent α-helix (Fig. 2*D*, *left panel*).

Deleting 45, 65, or 71 N-terminal amino acids had no effect, and I3 was inactive (Fig. 2*D*, *right panel*).

Leu^{108}, Leu^{109}, and Phe^{112} interact with the syndecan-1 core protein sequence GAGAL (24). Syndecan-1 is a cell surface heparan sulfate proteoglycan that mediates lacritin targeting of cells but only after heparanase (25) has exposed GAGAL nestled among heparan sulfate chains (24). Heparanase also generates heparan sulfate stubs that appear to be required for lacritin binding, suggesting a hybrid GAGAL/heparan sulfate binding site (24).

To assess the role of this interaction in restoration of homeostasis, we cultured cells overnight in xyloside to competitively suppress heparan and chondroitin sulfate assembly (35) (Fig. 2*E*, *left diagram*). We also attempted to deplete cells of syndecan-1 using shRNAs. Xyloside completely abrogated lacritin cytoprotective activity (Fig. 2*E*, *left panel*). However, syndecan-1 was resistant to knockdown with three individual or pooled syndecan-1 shRNAs (supplemental Fig. 1) unlike syndecan-1 siRNAs in human salivary gland/HeLa cells (25).

Xyloside can promote growth arrest and apparently lessen viability by reducing the synthesis of hyaluronan by UDP-glucuronyltransferase-dependent glucuronidation of xyloside to diminish available UDP-glucuronic acid (36). To determine whether the same may be true of xyloside on HCE-T cells, we considered the expression of UDP-glucuronyltransferase (UGT) genes. No human corneal UGT expressed sequence tags are apparent in NEIBank. Nonetheless, we attempted to amplify UGT1A6 transcripts from HCE-T cells by RT-PCR. No amplicons were detected (supplemental Fig. 1) in keeping with only a slight negative effect of xyloside on cell viability (Fig. 2*E*, *right panel*). Taken together, the capacity of tears to restore homeostasis is dependent on lacritin and specifically on a region in its C terminus that includes the syndecan-1 binding domain.

Lacritin Stimulates Rapid Autophagy—To elucidate how lacritin promotes homeostasis, we blotted for caspases 9 and 3 and observed some apoptotic cleavage coincident with IFNG/TNF stress (Fig. 3*A*). Thirty minutes of lacritin treatment had no effect on caspase cleavage but did substantially diminish the quantity of blottable macroautophagic marker LC3-II, which had also increased with stress (Fig. 3*A*). Decreased LC3-II is commonly indicative of macroautophagic inhibition (37) but conceptually might represent the opposite because blockers to force the accumulation of "autophagosomes" were not included.

Autophagy is a self-catabolic process (Fig. 3*B*) by which LC3-II-decorated "isolation membranes" and autophagosomes (Fig. 3*B*, *left*), respectively, envelop and enclose stress-damaged proteins and organelles (Fig. 3*B*, *middle*). Subsequent fusion with endosomes or lysosomes ("autolysosome"; Fig. 3*B*, *right*) initiates degradation (2), thereby helping to alleviate stress.

To first determine whether IFNG/TNF stimulates autophagic flux, blocking agents were introduced. Inhibition of autolysosomal content degradation or autophagosome-lysosome fusion by respective treatment of stressed cells with leupeptin (Fig. 3, *C* and *D*, *top*) or vinblastine (Fig. 3, *C* and *D*, *middle*) caused LC3-II to accumulate over 6 h in keeping with increased autophagic flux. In contrast, class 1 and 3 phosphatidylinositol-4,5-bisphosphate 3-kinase (PI3K) inhibitor wortmannin blocked the initiation of autophagy and the appearance of LC3-II (Fig. 3, *C* and *D*, *bottom*).

We compared flux 30 min after lacritin treatment in stressed cells without or with leupeptin. In the presence of leupeptin, LC3-II accumulated (Fig. 3, *E*, *bottom*, and *F*) at a level equivalent to 6 h without lacritin (Fig. 3, compare *F* with *D*). Similar results were obtained with bafilomycin as early as 10 min (not shown), suggesting that lacritin accelerates autophagic flux.

Because the sensitivity of LC3-II blotting is not optimal for monitoring autophagosomal accumulation over short times, we stably transduced HCE-T cells with LC3 double tagged with mCherry and EGFP (LC3/RG (28); Fig. 3*B*, *bottom left* and *top right*). Quenching of the EGFP signal in acidic lysosomal compartments distinguishes LC3 in isolation membranes and autophagosomes from LC3 in autolysosomes.

Cells were stressed with IFNG and TNF in the presence of lacritin or C-25 as above. Both tags were equally represented in C-25-treated cells (Fig. 3, *H* and *J*). However, in lacritin-treated cells, mCherry dominated as early as 10 min. Thereafter, it progressively decreased as proportionally did EGFP (Fig. 3, *G* and *K*). When lysosomal fusion was blocked by vinblastine, EGFP puncta accumulated (Fig. 3, *I*, *L*, and *M*). Together, these data suggest that lacritin rapidly accelerates autophagic flux coincident with the loss of detectable LC3-II with LC3-II degradation apparently exceeding biosynthesis.

Lacritin-stimulated Autophagy Is Necessary for Homeostasis and Is mTOR-independent—Lacritin triggers mitogenic phospholipase C/Ca^{2+}/calcineurin/NFATC1 and phospholipase C/phospholipase D/mTOR signaling in human salivary gland/HeLa cells (26). Activation of mTOR inhibits autophagy (38). We therefore monitored mTOR activity in HCE-T cells (Fig. 4, *A* and *B*) by blotting for phosphorylated ribosomal protein S6 kinase (RPS6KB1 or "S6K"), which in turn promotes cell proliferation and protein synthesis. With or without stress, mTOR was constitutively active and statistically similar in the absence or presence of lacritin (Fig. 4, *A* and *B*), although IFNG and TNF suppress S6K phosphorylation in insulin-like growth factor 1-stimulated C2C12 mouse myoblast cells (39).

Lacritin-dependent rescue of stressed HCE-T cells was not enhanced by inclusion of rapamycin or class 1 PI3K inhibitor PI103 (Fig. 4*C*). Other mediators of lacritin mitogenic signaling include Ca^{2+}, downstream calcineurin, and NFATC1. Increased intracellular Ca^{2+} stimulates autophagy (40). We therefore challenged stressed cells with the calcineurin inhibitor cyclosporin A in the presence of lacritin. Cyclosporin A was completely inhibitory (Fig. 4*C*). A constitutively active calcineurin splice variant blocks FOXO activation in muscle (41). Lacritin also inactivates FOXO3 by forcing it into the cytoplasm (Fig. 1, *I* and *M*).

Is lacritin-stimulated autophagy necessary for homeostasis? We targeted ATG7 mRNA for degradation by shRNA (Fig. 4*D*). ATG7 is a ubiquitin-like E1 activating enzyme that is essential for autophagy as part of the LC3 lipidation system (42). HCE-T cells were stably transduced with one of three different ATG7 shRNAs or with an empty vector control ("shCtrl"). ATG7 became depleted (Fig. 4*E*), and lacritin-dependent survival (Fig. 4*D*) and FOXO3 translocation (Fig. 4*F*) were abrogated or diminished.

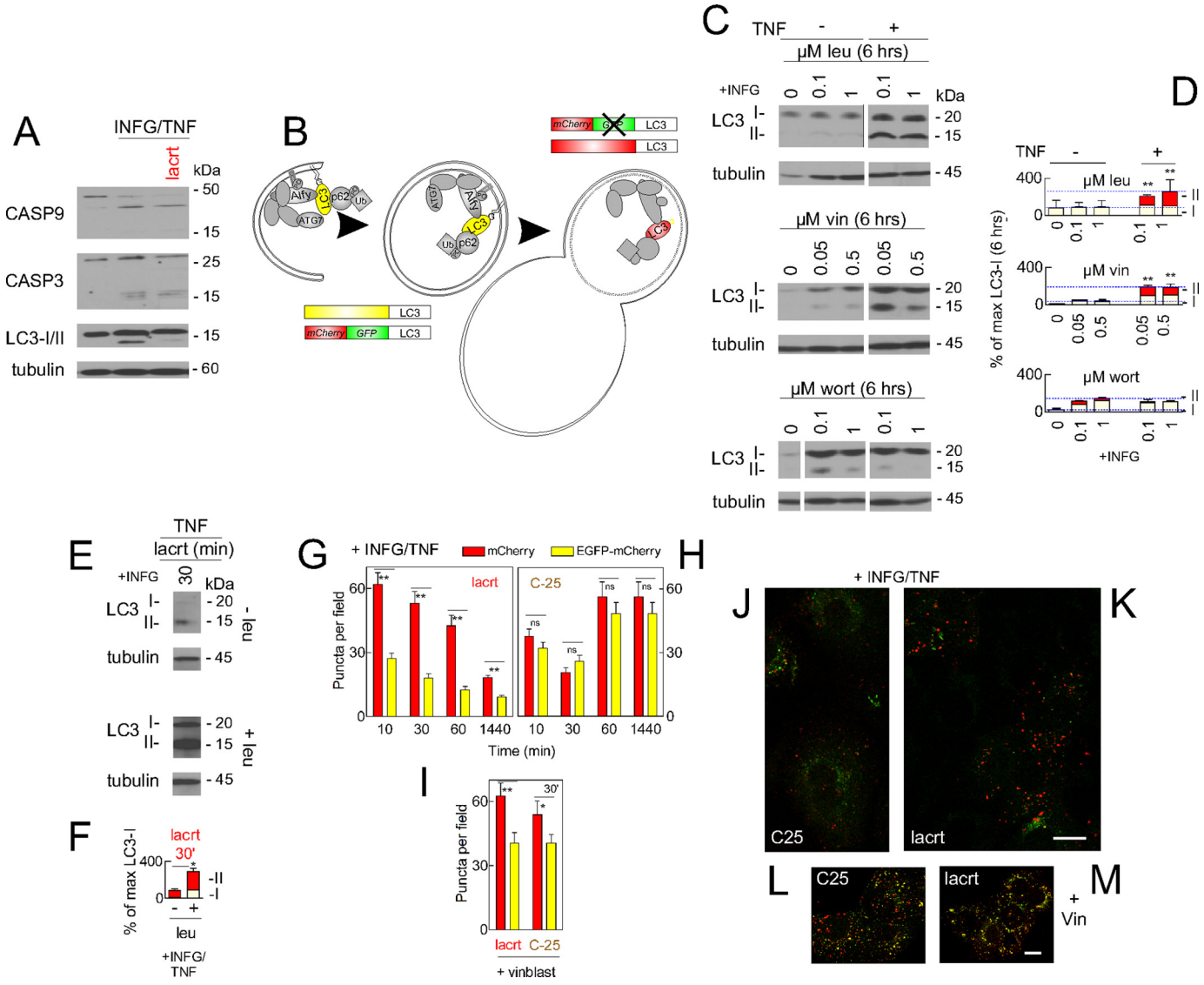

FIGURE 3. **Stressed cells display enhanced autophagy that is further up-regulated by lacritin within 10 min.** *A*, HCE-T cells were either not stressed or were stressed overnight with IFNG and then treated for 30 min without or with lacritin (10 nM) in the presence of TNF. Cell lysates were blotted for caspases (*CASP*) 9 and 3 or for LC3 and tubulin (loading control). LC3-I migrates more slowly than LC3-II. *B*, schematic diagram of autophagy with isolation membrane (*left*), autophagosome (*center*), autolysosome (*right*), and several autophagy mediators (LC3, ATG7, Alfy, and p62). HCE-T cells that stably express LC3 double tagged with EGFP and mCherry (22) were developed (LC3/RG cells) and used in *G–M* to monitor autophagic flux. *Rectangles* indicate the effect of pH on LC3 tags. *C*, HCE-T cells were sensitized overnight with IFNG and then treated for 6 h without or with TNF in the presence of no or increasing amounts of leupeptin (*leu*), vinblastine (*vin*), or wortmannin (*wort*). Lysates were blotted for LC3 or tubulin (loading control). *D*, autophagic flux is chronically enhanced by TNF stress as revealed by accumulation of LC3-II with leupeptin and vinblastine. Each value plotted is the mean integrated optical density of the films ($n = 3$) normalized to the tubulin loading control. *E*, HCE-T cells were sensitized overnight with IFNG and then treated for 30 min with lacritin (10 nM) in the presence of TNF without or with 0.1 μM leupeptin. Lysates were blotted for LC3 or tubulin (loading control). *F*, quantitation of replicate experiments from *E* (paired *t* test for LC3-II; *, $p < 0.05$) plotted as indicated in *D*. LC3/RG cells were sensitized overnight with IFNG and then treated for different times with 10 nM lacritin (*G*) or C-25 in the presence of TNF without (*H*) or with 0.05 μM vinblastine (*vinblast*) (*I*). Puncta per field in microscopic images were quantitated (ANOVA with Dunnett's post-test; **, $p < 0.01$; *, $p < 0.05$; *ns*, not significant). Representative microscopic images are shown in *J–M*. *J*, C-25 for 60 min. *K*, lacritin for 60 min. C-25 (*L*) and lacritin (*M*) treatment for 60 min in the presence of vinblastine (*Vin*; 0.05 μM) is shown. *Bar*, 10 μm. *Error bars* represent S.E.

For accelerated autophagic flux to promote homeostasis, it must be transient because excessive autophagy appears to be coincident with death (2). We scrutinized endogenous LC3-II more precisely in time and with different lacritin doses, all without autophagy blockers. Within 1 min of lacritin treatment, LC3-II was poorly detectable (Fig. 4*G*, *upper panel*, and *H*), but by 24 h, LC3-II was equivalent to the C-25 negative control (Fig. 4*I*, *lower panel*, and *J*). The lacritin response is biphasic with a dose optimum of 10 nM (Fig. 4*I*, *upper panel*, and *J*), thus mirroring the viability response (Fig. 1*L*, *left panel*). In contrast, C-25 was ineffective at all times and doses (Fig. 4*G*, *lower half*; *H*; *I*, *lower panel*; and *J*). Taken together, lacritin-stimulated restoration of homeostasis is dependent on autophagy in an mTOR-independent manner that is rapid and transient.

Lacritin-stimulated Autophagy Diverts Htt103Q-mCFP—Growth factor-accelerated autophagy is unusual. Yamamoto *et al.* (43) observed insulin-like growth factor 1-stimulated autophagic clearance of aggregated mutant huntingtin Gln_{65} and Gln_{103} proteins (Htt65 and Htt103Q, respectively) over 3 days in normal HEK293 cells. Transient and rapid autophagy

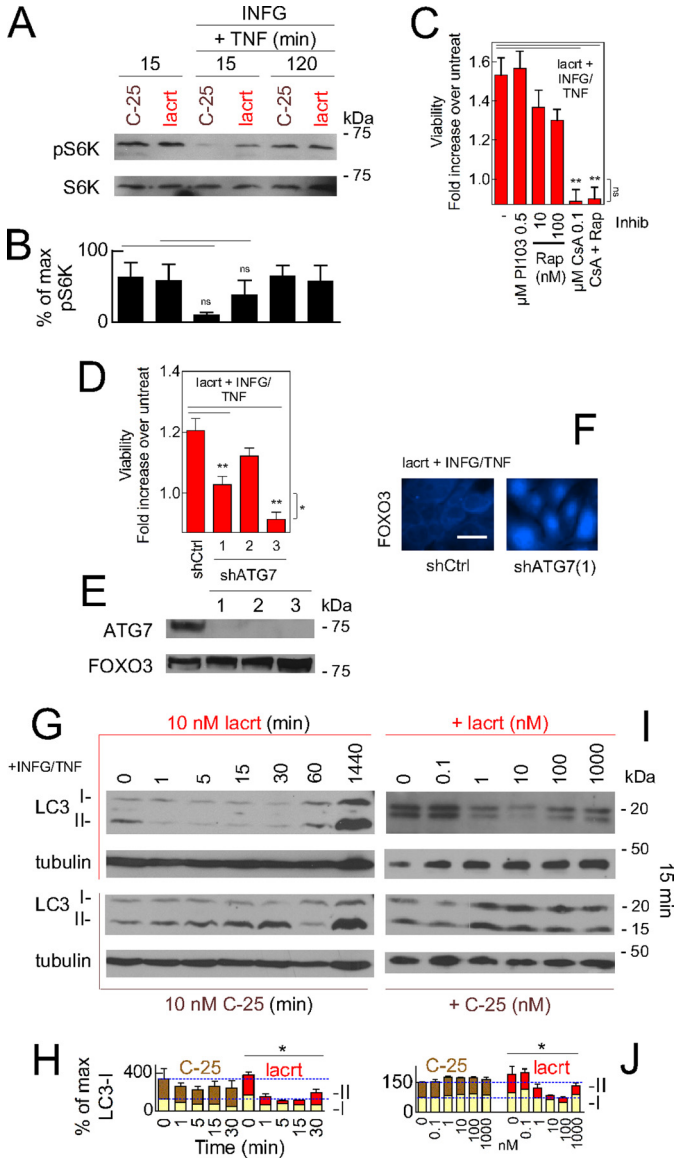

FIGURE 4. **Lacritin-stimulated autophagy is calcineurin- but not mTOR-dependent and necessary for cell survival.** *A*, HCE-T cells were either not stressed or alternatively were stressed overnight with IFNG and then treated for 15 or 120 min with 10 nM lacritin or C-25 in the absence or presence of TNF. Cell lysates were blotted for phospho-S6K or S6K (loading control). Phospho-S6K is an indicator of mTOR activity. *B*, quantitation of replicate experiments from *A* (paired *t* test; *ns*, not significant, $p > 0.05$). Each value plotted is the mean integrated optical density of the films ($n = 3$) normalized to the S6K loading control. *C*, HCE-T cells were stressed overnight with IFNG and then treated for 15 min with 10 nM lacritin in the presence of TNF without or with PI103, rapamycin (*Rap*), cyclosporin A (*CsA*), or rapamycin plus cyclosporin A. Viability was assessed by the MTT assay and is expressed as the -fold increase in viability, defined as the ratio of experimental viability to the control viability. Control viability was derived from cells treated with IFNG/TNF alone (ANOVA with Dunnett's post-test; **, $p < 0.01$). Viability with 0.1 μM cyclosporin A or 0.1 μM cyclosporin A and rapamycin treatment plus IFNG/TNF and lacritin does not significantly differ from viability of cells treated with IFNG/TNF alone (ANOVA with Dunnett's post-test; *ns*, not significant, $p > 0.05$). *D*, HCE-T cells stably expressing empty vector (shCtrl) or three different ATG7 shRNAs were developed. Each was stressed overnight with IFNG and then treated for 15 min with 10 nM lacritin in the presence of TNF. Viability was assessed by the MTT assay and is expressed as the -fold increase in viability as defined above (ANOVA with Dunnett's post-test; **, $p < 0.01$). Viability from shATG7(3) cells with IFNG/TNF and lacritin differs significantly from shCtrl cells treated with IFNG/TNF alone (*t* test; *, $p = 0.03$); thus, shATG7(1) was used in subsequent experiments. *E*, Western blot for ATG7 in shCtrl and shATG7 knockdown cell lines using FOXO3 as a loading control. *F*, shCtrl or shATG7(1) HCE-T cells were sensitized overnight with IFNG and then treated for 15 min with lacritin (10 nM) in the presence of TNF. Cells were washed and fixed, and then FOXO3 was immunolocalized. *G*, HCE-T cells were sensitized overnight with IFNG and then treated for different times with 10 nM lacritin (*top pair*) or C-25 (*bottom pair*) in the presence of TNF. Lysates were blotted for LC3 or tubulin (loading control). *H*, quantitation of *G* replicates plotted as indicated in *B* normalized to the tubulin loading control. *I*, HCE-T cells were sensitized overnight with IFNG and then treated for 15 min with different doses of lacritin (*top pair*) or C-25 (*bottom pair*) in the presence of TNF. Lysates were blotted for LC3 or tubulin. *J*, quantitation of *I* replicates plotted as indicated in *H*. *H* and *J*, two-way ANOVA (LC3-II and LC3-I); *, $p < 0.05$. *Error bars* represent S.E. *Inhib*, inhibitor; *lacrt*, lacritin; *pS6K*, phospho-S6K.

might capture IFNG/TNF-damaged proteins at a level sufficient to rescue cell viability.

To examine capture directly, we transiently overexpressed huntingtin mutant Htt103Q-mCFP or Htt25Q-mCFP (Fig. 5) in LC3/RG cells and monitored autophagy without IFNG/TNF. Whereas colocalization of the mCherry tag with toxic Htt103Q-mCFP steadily rose with C-25 (Fig. 5, *B* and *F*), lacritin triggered a peak of enhanced colocalization at 30 min (Fig. 5, *B* and *E*), suggesting transiently accelerated capture of Htt103Q in autolysosomes. The number of mCherry- and mCFP-labeled puncta also peaked at 30 min but not with C-25 (Fig. 5, *C* and *D*) for which the number of puncta declined at 60 min. Autophagic flux was unchanged in Htt25Q cells despite the presence of lacritin (Fig. 5, *B*, *C*, *G*, and *H*), suggesting that stress is a prerequisite for lacritin-stimulated autophagy.

To determine how lacritin-triggered capture might be mediated, we considered the involvement of Alfy (WDFY3) and p62 (SQSTM1). Alfy shuttles from the nuclear membrane to target phosphatidylinositol 3-kinase-generated phosphatidylinositol 3,4,5-trisphosphate in isolation membranes and binds aggregated proteins (29). p62 is an efficient ubiquitin-binding protein (44, 47). Both interact with LC3 and thus play an important role recruiting aggregated and polyubiquitinated proteins and organelles to isolation membranes for autophagic degradation (28, 29). We monitored LC3-Alfy and LC3-p62 coupling soon after lacritin or C-25 treatment. None was detected at time 0; however, within 1 min of lacritin addition, both Alfy and p62 bound LC3 (Fig. 6*A*). Binding was maximal by 1 or 5 min, thereafter subsiding (Fig. 6, *A*, *C*, and *D*), and coincided in part with stimulated LC3 capture of polyubiquitinated proteins (Fig. 6, *A*, *upper bracket*, and *E*). Capture was first apparent at 5 min and continued to 15 min (Fig. 6, *A* and *E*, *lower*). In contrast, C-25 had no stimulatory effect (Fig. 6, *B* and *C–E*). Free polyubiquitin chains of apparently three to nine units (21–63 kDa, respectively; Fig. 6*A*, *lower bracket*) also seemed to slightly increase with lacritin, although many were already transiting into autophagosomes (Fig. 6*A*) and were detected in C-25-treated cells (Fig. 6*B*, *lower*). Unanchored chains may be a consequence of TNF signaling to the ubiquitin ligase TRAF6 (45) because TRAF6 together with UBC13 (ubiquitin-conjugating enzyme E2N (UBE2N)) and UEV1A (ubiquitin-conjugating enzyme E2 variant 1 (UBE2V1)) catalyze polyubiquitination on Lys^{63} (46). Thus, stress is a prerequisite for lacritin-stimulated autophagy that effectively captures aggregated and ubiquitinated proteins for degradation using Alfy and p62.

Autophagy and Metabolism—Autophagy appears to be upstream of the tricarboxylic acid cycle and oxidative phosphorylation (48, 49). Does lacritin-stimulated autophagy influence

cellular metabolism? We compared the basal oxygen consumption rates of stressed cells treated with lacritin or C-25 and then dissected the source of oxygen consumption by sequential treatment with oligomycin and FCCP followed by rotenone and antimycin A (49). Oligomycin blocks oxidative phosphorylation by inhibiting ATP synthase. FCCP transports protons across the inner mitochondrial membrane to stimulate electron transport and enhance oxidative phosphorylation. Rotenone

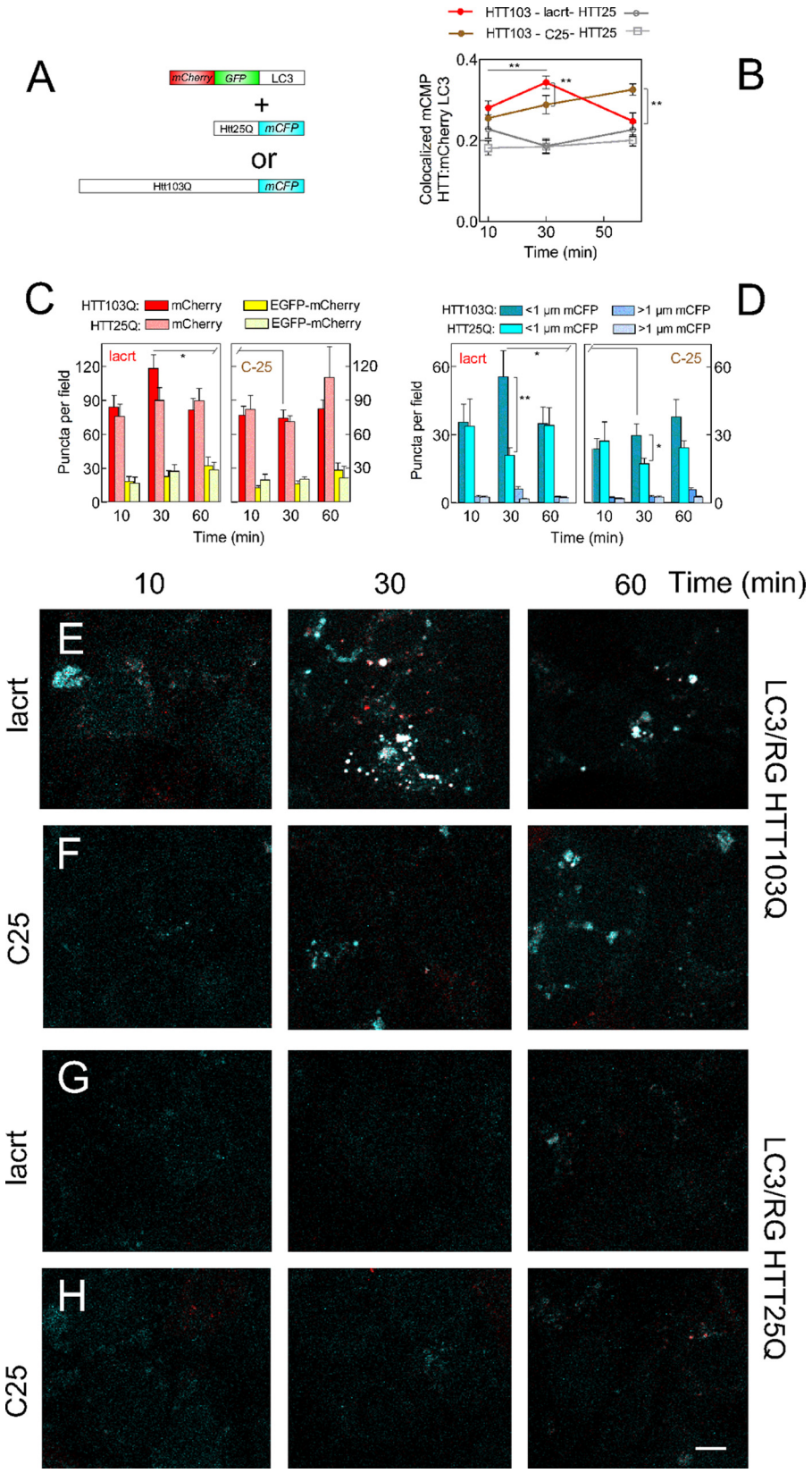

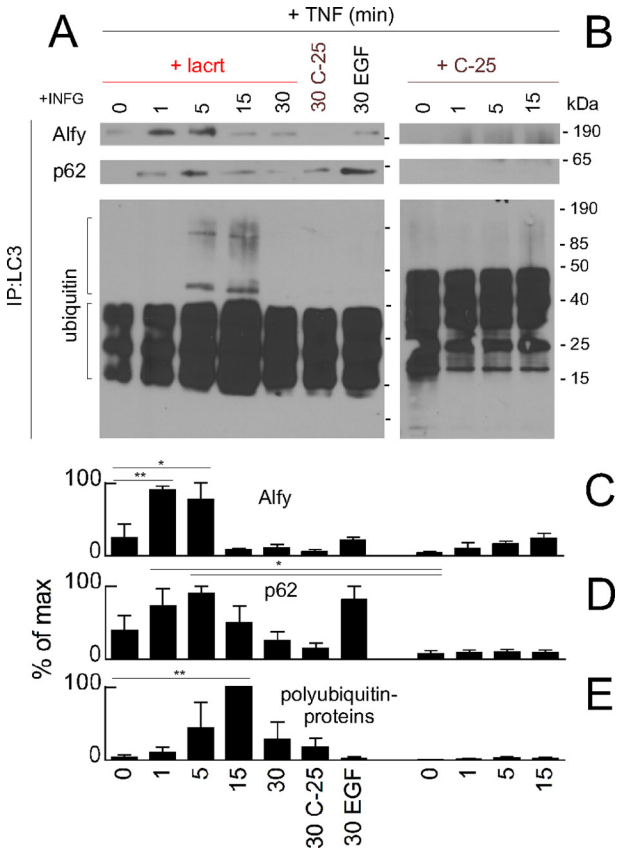

FIGURE 6. **Lacritin-stimulated autophagic capture with p62 and Alfy.** *A*, HCE-T cells were stressed overnight with IFNG and then treated for different times with 10 nM lacritin or for 30 min with 10 nM C-25 or EGF (1 μg/ml) in the presence of TNF. LC3 was immunoprecipitated (*IP*) from cell lysates. Immunoprecipitated material was blotted for Alfy, p62, or ubiquitin. *B*, same as *A* in which cells were treated with 10 nM C-25 for different times. *C–E*, quantitation of *A* and *B* with replicates (ANOVA with Dunnett's post-test; *, $p < 0.05$; **, $p < 0.01$). Each value plotted is the mean integrated optical density of the films ($n = 3$). *lacrt*, lacritin.

and antimycin A shut down oxygen consumption by blocking electron transport. Within 8 min of lacritin treatment, basal oxygen consumption had increased (Fig. 7, *A* and *B*). ATP-linked oxygen consumption, the maximal respiratory rate, and "spare respiratory capacity" were also increased (Fig. 7*B*).

Spare respiratory capacity is the difference between basal and maximal oxygen consumption. Greater spare respiratory capacity reduces sensitivity to stress. Spare respiratory capacity can be acquired over several days of mitochondrial biogenesis (50) or by mitochondrial fusion (51). We therefore monitored mitochondrial fusion in stressed cells that had taken up Mito-Tracker Red and observed more fusion events per second in lacritin-treated cells than in those receiving C-25 (Fig. 7, *C* and *D*). This effect was abrogated by ATG7 shRNA depletion (Fig. 7*C*), suggesting that accelerated autophagy was upstream of enhanced spare respiratory capacity and mitochondrial fusion.

FOXO3 and autophagy are important regulators of cellular metabolism (37). We performed an unbiased metabolomic study of stressed HCE-T cells that followed 135 metabolites. Ten minutes of lacritin treatment significantly altered the levels of 29 metabolites (Fig. 7*E*) in ways suggesting augmented oxidative phosphorylation (decreased glutamate and glutamine (52)) and decreased protein aggregation (decreased kynurenine (53)). Enhanced acetylation could be implied by partial exhaustion of 1-methylnicotinamide (54), coenzyme A as acetyl-CoA (55), and precursor pantothenate and by the apparent utilization of spermine and spermidine.

FOXO1, FOXO3, and Acetylation—Acetylation can serve as an autophagy switch. Hypoacetylation of histone H3 by exogenous spermidine transcriptionally promotes autophagy (56). Recently, cytoplasmic FOXO1 was reported to become acetylated with stress and as a consequence to ligate ATG7 and stimulate autophagy (5). We detected stress-associated acetylation of FOXO1 (Fig. 8, *A* and *B*) but unexpectedly no bound ATG7 (Fig. 8, *A* and *B*). Bound ATG7 was detected only after cells were treated with lacritin (Fig. 8, *C–F*). The interaction was maximal 5–15 min after lacritin treatment. However, only 1 min was sufficient to diminish the quantity of detectable LC3-II (Fig. 4, *G* and *H*), suggesting that FOXO1-ATG7 coupling was not the primary initiator of lacritin-accelerated autophagy.

We therefore explored the possibility that FOXO3 acetylation might be involved. Hyperacetylation of FOXO3 was detected 1 min after lacritin addition (Fig. 8, *G* and *H*), and FOXO3 remained acetylated for at least 15 min. By 60 min, it was largely absent (Fig. 8, *G* and *H*). A lower level of stress-associated acetylation (57) was apparent in C-25-treated cells. No binding was observed to ATG7 (Fig. 8, *G* and *H*), ATG3, ATG4B, or ATG12 (not shown).

The autophagy proteomic network provided evidence for an interaction with ATG101 (C12orf44) (58), and indeed FOXO3 affinity precipitates contained ATG101 within 1 min of lacritin treatment (Fig. 8, *I–K*). No interaction was observed in C-25-treated cells (Fig. 8, *J* and *K*). ATG101 coupling of ATG13 stabilizes the ULK1-ATG13 complex (Fig. 9*A*) (22, 23) necessary for the initiation of autophagy. Knockdown of ATG101 abrogates autophagy (22, 23).

To determine whether ATG101 was essential for lacritin-stimulated autophagy, HCE-T cells were stably transduced with individual or pooled ATG101 shRNAs (Fig. 9*B*). Empty vector cells (shCtrl) or C-25-treated cells served as controls. Diminishment of LC3-II with lacritin was completely hindered by pooled shATG101s (Fig. 9, *C* and *D*), suggesting that lacritin-stimulated autophagy was interrupted. Cells were next stably transduced with each of three different FOXO3 shRNAs or with empty vector (Fig. 9*E*). Each shFOXO3 was effective, and lacritin restoration of homeostasis was abrogated (Fig. 9*F*).

FIGURE 5. **Lacritin-stimulated autophagy captures Htt103Q cellular aggregates.** *A*, Htt103Q-mCFP or Htt25Q-mCFP constructs transduced in HCE-T cells stably expressing LC3 double tagged with EGFP and mCherry (22) (LC3/RG cells). *B*, quantitation of colocalized mCFP-Htt and mCherry LC3 at different times after treatment with 10 nM lacritin or C-25 in the absence of IFNG and TNF (*t* test; **, $p < 0.01$). *C*, number of LC3 mCherry- or LC3 mCherry-EGFP-labeled puncta in cells expressing Htt103Q or Htt25Q at different times after treatment with 10 nM lacritin or C-25 (no IFNG/TNF) (*t* test; *, $p < 0.05$). *D*, number of Htt103Q or Htt25Q puncta greater or less than 1 μm at different times after treatment with 10 nM lacritin or C-25 (no IFNG/TNF) (*t* test; *, $p < 0.05$; **, $p < 0.01$). Representative microscopic images are shown in *E–H*. *E* and *F*, LC3/RG cells expressing Htt103Q-mCFP that were treated with lacritin (*E*) or C-25 (*F*) for different times. Cells were washed and fixed, and all tags were localized. IFNG/TNF was omitted. *G* and *H*, LC3/RG cells expressing Htt25Q-mCFP that were treated with lacritin (*G*) or C-25 (*H*) for different times. IFNG/TNF was omitted. *Bar*, 10 μm. *Error bars* represent S.E. *lacrt*, lacritin.

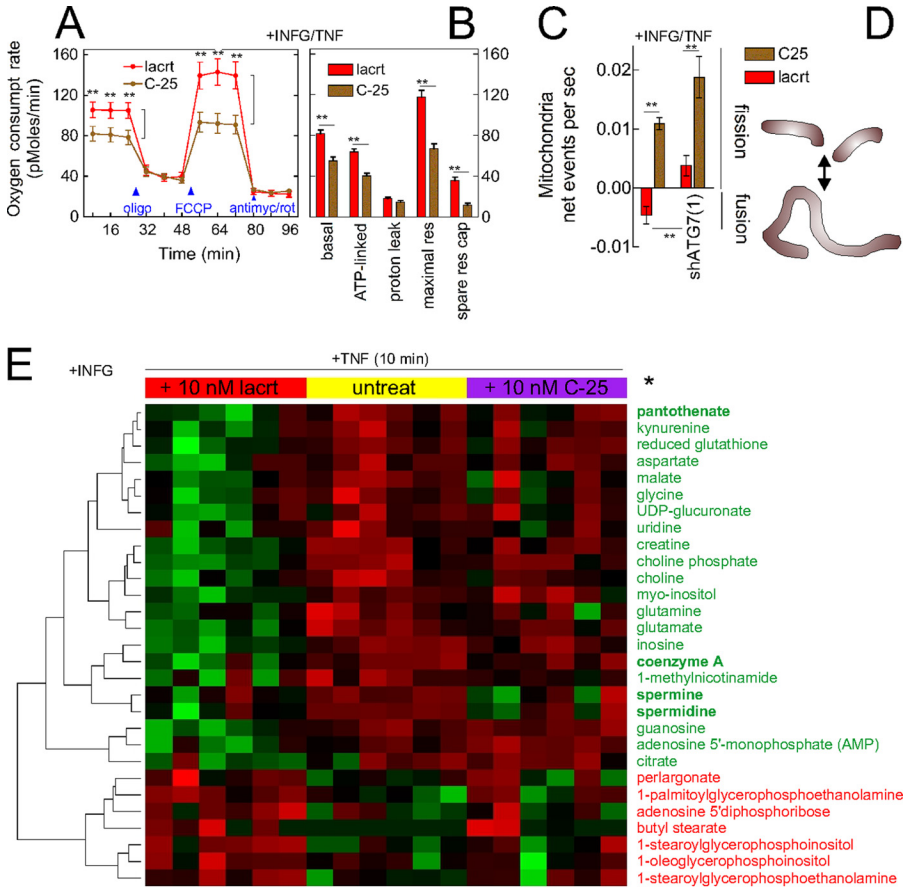

FIGURE 7. **Lacritin restores metabolism.** *A*, HCE-T cells were stressed overnight with IFNG and then treated for different times with 10 nM lacritin or C-25 in the presence of TNF. The oxygen consumption rate was monitored in the absence or presence of oligomycin (500 nM), FCCP (375 nM), or antimycin A (750 nM) and rotenone (1 μM) together. *B*, features of the oxygen consumption rate as revealed by use of oligomycin, FCCP, antimycin A, and rotenone (*t* test; **, $p < 0.01$). *C*, HCE-T or HCE-T shATG7(1) cells were stressed overnight with IFNG and then stained for 30 min with MitoTracker Red FM. After addition of lacritin or C-25 (10 nM) in the presence of TNF, live mitochondria were monitored at 20-s intervals for 30 min, and fission frequency was estimated from ComponentCount of Mytoe. *D*, schematic diagram of mitochondrial fusion or fission. *E*, HCE-T cells were stressed overnight with IFNG and then treated for 10 min in replicates of six with 10 nM lacritin or C-25 or left untreated in the presence of TNF. Metabolites in cell lysates were identified by mass spectrometry. Values were analyzed by the *t* test and non-parametric Wilcoxon test of the log-transformed normalized data (*, $p < 0.05$) and further analyzed by hierarchical clustering. *Error bars* represent S.E. *lacrt*, lacritin; *antimyc*, antimycin A; *rot*, rotenone; *res*, respiration; *res cap*, respiratory capacity; *untreat*, untreated.

If FOXO3 is an important mediator, then dominant negative FOXO3 (FOXO3Nt) should stimulate homeostasis in the absence of lacritin. FOXO3Nt interferes with the capacity of endogenous FOXO3 to bind DNA and initiate transcription for cell stress or death (59), thus likely making more cytoplasmic FOXO3 available. We transduced cells with FOXO3Nt and then stressed them with IFNG/TNF. Like lacritin, FOXO3Nt restored homeostasis (Fig. 9*F*).

DISCUSSION

How homeostasis is regulated in stress is a key question in biology. We report a new process in which the prosecretory mitogen lacritin rapidly restores homeostasis to stressed epithelia through an immediate and novel acceleration of autophagy that diverts aggregated proteins for degradation and quickly promotes oxidative phosphorylation. Accelerated flux appears to be initiated by lacritin-stimulated acetylation of FOXO3 as a novel ATG101 ligand and involves kinetically slower lacritin-dependent coupling of stress-acetylated FOXO1 with ATG7.

That lacritin-depleted tears were not partially compensated by other tear factors was unexpected. Tears contain EGF, glial cell-derived neurotrophic factor, hepatocyte growth factor, mucin 4 (cell surface-associated), neurotrophin 3, neurotrophin 5 (60), and transforming growth factor β1 (61) as well as numerous chemokines, proteases, protease inhibitors, Igs, lipids, carrier proteins, and adhesion factors (60). Several of these tear factors have demonstrated corneal epithelial mitogenic activity and in some cases promote corneal angiogenesis (60). However, only glial cell-derived neurotrophic factor overexpression (62) and exogenous hepatocyte growth factor (63) are known to support the survival of stressed corneal epithelial cells. Levels of each may be low. Glial cell-derived neurotrophic factor is a product of both the cornea and lacrimal gland (NEIBank), but no hepatocyte growth factor transcripts are detected in either tissue or in the conjunctiva (NEIBank). In contrast, lacritin is the sixth most common lacrimal gland transcript (64) and has been detected in the Meibomian gland proteome and by PCR in cornea (34). Fleiszig *et al.* (65) suggested previously that tears offer epithelial protection from infection

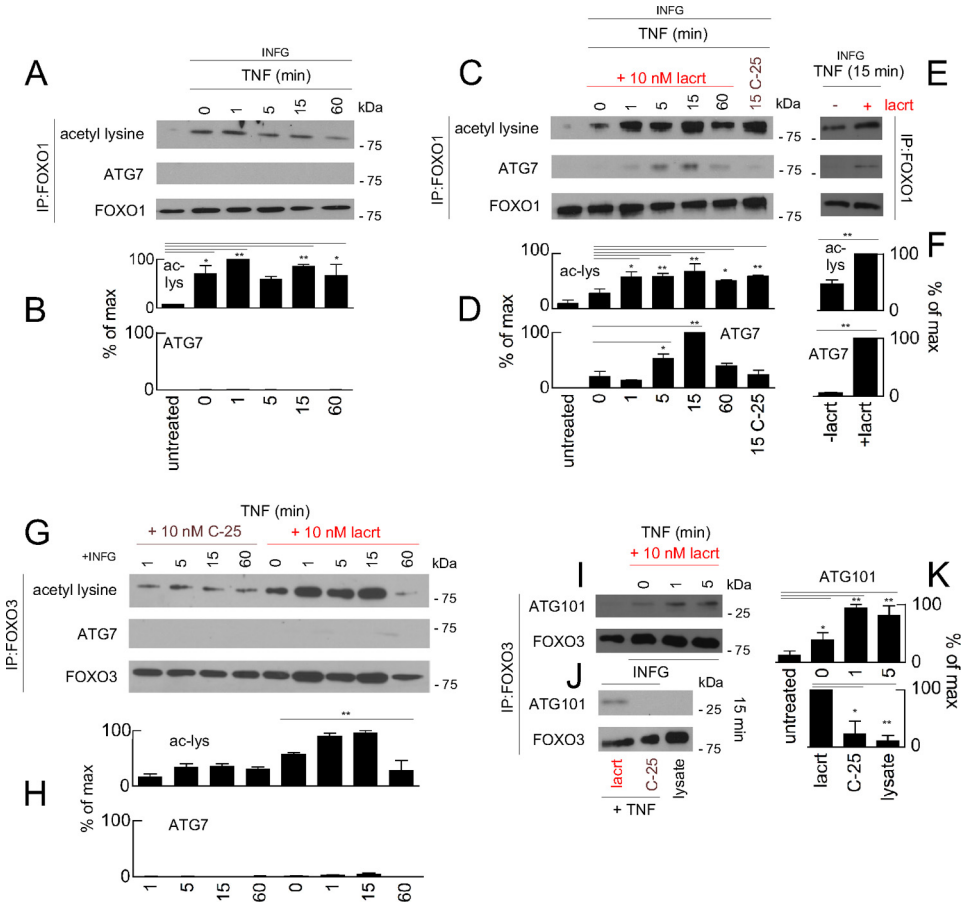

FIGURE 8. **Lacritin stimulated FOXO1-ATG7 and FOXO3-ATG101 coupling.** *A*, HCE-T cells were either not stressed or stressed overnight with IFNG and treated for different times with TNF. FOXO1 was immunoprecipitated (*IP*) from cell lysates, and the immunoprecipitated material was blotted for acetyl-lysine, ATG7, or FOXO1 (loading control). *B*, quantitation from replicate blots (ANOVA with Dunnett's post-test; *, $p < 0.05$; **, $p < 0.01$). Each value plotted is the mean integrated optical density of the films ($n = 3$) normalized to the FOXO1 loading control. *C*, same as *A* in which stressed cells were also treated with 10 nM lacritin or C-25. *D*, quantitation from replicate blots (ANOVA with Dunnett's post-test; *, $p < 0.05$; **, $p < 0.01$) plotted as indicated in *B*. *E*, replicate blot of the 15-min time point from *C* without or with lacritin. *F*, quantitation of replicate blots from *E* plotted as indicated in *B* (*t* test; **, $p < 0.01$). *G*, HCE-T cells were either not stressed or stressed overnight with IFNG and treated for different times with TNF. FOXO3 was immunoprecipitated from cell lysates, and the immunoprecipitate was blotted for acetyl-lysine, ATG7, or FOXO3 (loading control). *H*, quantitation from replicate blots (ANOVA; **, $p < 0.01$) plotted as indicated in *B* but normalized to the FOXO3 loading control. *I*, HCE-T cells were either not stressed or stressed overnight with IFNG and treated for different times with 10 nM lacritin in the presence of TNF. FOXO3 was immunoprecipitated from cell lysates. Immunoprecipitated material was blotted for ATG101 or FOXO3 (loading control). *J*, replicate blot of the 15-min time point from *I* with 10 nM lacritin, C-25, or lysate alone. *K*, quantitation from replicate blots (ANOVA with Dunnett's post-test; *, $p < 0.05$; **, $p < 0.01$) plotted as indicated in *H*. *Error bars* represent S.E. *lacrt*, lacritin; *ac-lys*, acetyl-lysine.

independently of its antimicrobial activity. Here we show that tears effectively substitute for the cornified barrier in skin, and lacritin may be the master protector.

Mutual interaction of lacritin C and syndecan-1 N termini is important for survival. However, not all lacritin C-terminal point mutants shared survival and syndecan-1 binding activities. I98S and F104S lacritins were partially or completely inactive but displayed no altered affinity for syndecan-1 (24). Conversely, I73S lacritin failed to bind syndecan-1 (24) but was fully active. We suggest that each might interact with a second cell surface protein. Mitogenic signaling and autophagic stimulation by lacritin are pertussis toxin (26)- and MK912[3]-inhibitable, respectively, suggesting involvement of a G-protein-coupled receptor, possibly the α_{2c}-adrenergic receptor. siRNA knockdown and binding,[4] but not β-annexin-dependent reporter,[5] studies support this possibility, although prior coupling of α_{2c}-adrenergic receptor with a peptide or protein agonist has not been demonstrated. It was also noteworthy that the novel C-terminal domain (lacritin I3) of the lacritin-c splice variant was completely inactive and thus if differentially upregulated would not benefit the eye. Thus, although cell surface binding may involve more than just syndecan-1, both survival and cell targeting require lacritin hydrophobic residues Leu^{108}-Leu^{109}-Phe^{112} as a suitable binding face for the latent GAGAL domain of syndecan-1 (24). This emphasizes the importance of the unique heparanase-dependent targeting mechanism of lacritin that by exposing GAGAL transforms a ubiquitous cell surface proteoglycan into a localized lacritin-binding protein (25) necessary for survival when cells are stressed or mitogenesis (26) when not.

Characteristics of lacritin-accelerated autophagy are novel and informative. Diminished levels of detectable LC3-II might

[3] N. Wang and G. W. Laurie, unpublished data.
[4] P. Ma and G. W. Laurie, unpublished data.
[5] F. Velez and G. W. Laurie, unpublished data.

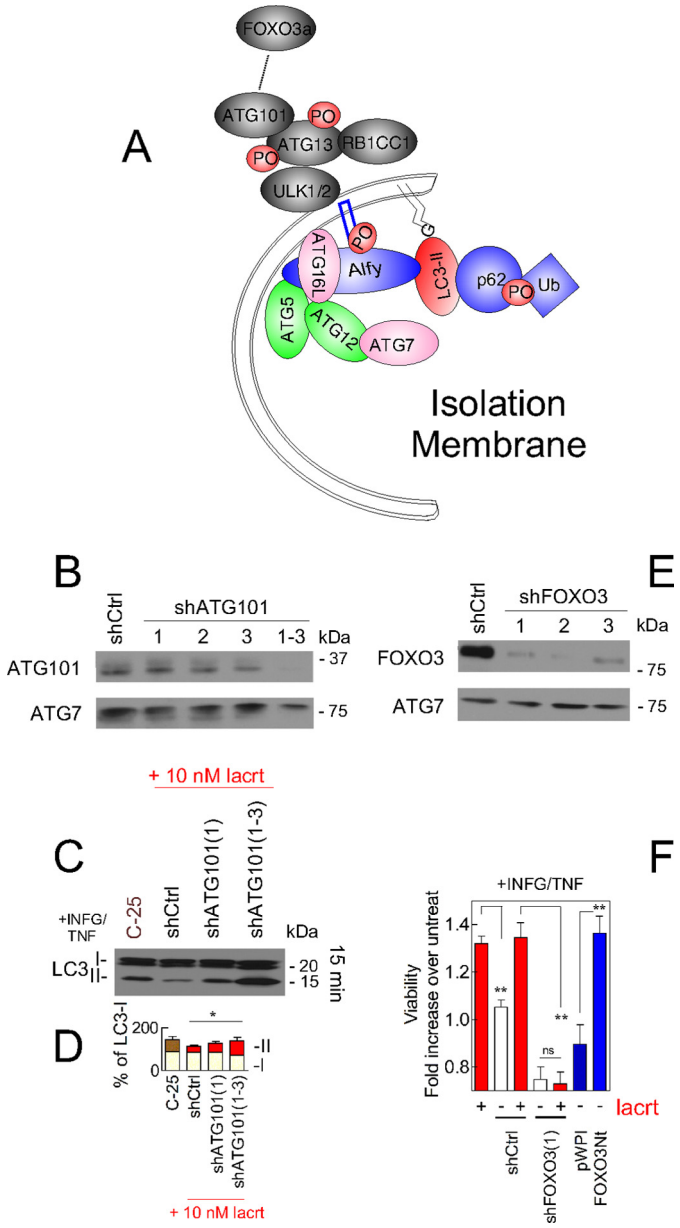

FIGURE 9. **FOXO3 and ATG101 are essential for lacritin stimulated autophagy.** *A*, schematic diagram of the isolation membrane illustrating several associated autophagic mediators. *B*, ATG101 immunoblot of stably transduced shCtrl, shATG101(1), shATG101(2), shATG101(3), or shATG101(1–3) HCE-T cells. ATG7 was used as a loading control. *C*, HCE-T and stably transduced HCE-T shCtrl, shATG101(1), and shATG101(1–3) cells were stressed overnight with IFNG and then treated for 15 min with 10 nM lacritin or C-25 in the presence of TNF. Lysates were blotted for LC3. *D*, quantitation of replicates from *B* (ANOVA for LC3-II; *, $p < 0.05$). Each value plotted is the mean integrated optical density of the films ($n = 3$) normalized to the tubulin loading control. *E*, FOXO3 immunoblot of stably transduced shCtrl, shFOXO3(1), shFOXO3(2), and shFOXO3(3) cells. ATG7 was used as a loading control. *F*, HCE-T, shCtrl, shFOXO3(1), pWPI, and FOXO3Nt cells were stressed overnight with IFNG and incubated for 15 min with TNF in the absence or presence of 10 nM lacritin. For comparison, HCE-T cells were transduced with pWPI vector or with FOXO3Nt (in pWPI). Cells were stressed overnight with IFNG and incubated for 15 min with TNF without lacritin. Viability was assessed by the MTT assay and is expressed as the -fold increase in viability, defined as the ratio of experimental viability to the control viability. Control viability was derived from cells treated with IFNG/TNF alone (*t* test; **, $p < 0.01$; *ns*, not significant, $p > 0.05$). *Error bars* represent S.E. *lacrt*, lacritin; *Ub*, ubiquitin; *untreat*, untreated.

be interpreted as inhibition of autophagy as is the case for cardiotrophin-like cytokine factor 1, FGF2, insulin-like growth factor 1, leukemia inhibitory factor, and SDF1 (CXCL12) in stressed or non-stressed cells (37) that signal through PI3K to activate mTOR. However, lacritin mitogenic mTOR signaling (26) is suppressed by IFNG/TNF stress. In the context of sudden increased autophagic flux (indicated by double tagged LC3 and accumulation of LC3-II with leupeptin), it appears that generation of LC3-II is rate-limiting and exceeded by degradation in keeping with the progressive decrease of EGFP-detected LC3 with lacritin addition.

Most studies follow autophagic flux for hours or a day in which inhibitors leupeptin, vinblastine, and E64D (37) are introduced to accumulate LC3-II as a measure of increased autophagic flux (66). That autophagy was initiated apparently within 1 min was made possible by the rapidity of lacritin-stimulated FOXO3 acetylation and associated coupling with ATG101 and LC3 recruitment of Alfy and p62 (as well as their cargo). shRNA depletion validated the importance of FOXO3 and ATG101, although much yet remains to be learned about their interactions.

Within the short times examined, for example, lacritin enhanced the level of detectable p62, whereas p62 is degraded over hours or a day of autophagy (66). Enhanced p62 may represent exposure of sequestered p62 whose availability might elevate the capacity for polyubiquitinated protein capture and degradation by autophagy and possibly by the proteasome with which p62 interacts (67). This might explain the differing kinetics of LC3/p62- and p62-dependent capture. It is also possible that by elevating p62 lacritin might trigger NF-κB survival signaling as previously noted for Ras (68).

Growth factor- or hormone-stimulated autophagy is effective and widely relevant. Insulin-like growth factor 1 promotes the autophagic clearance of aggregated mutant huntingtin Gln_{65} and Gln_{103} proteins (Htt65 and Htt103Q, respectively) in normal HEK293 cells (43). The adipocyte hormone and metabolic regulator leptin triggers autophagy in HeLa cells and in mouse kidney, liver, heart, and muscle (66). IL-1β-induced autophagy kills *Mycobacterium tuberculosis* in infected macrophages over 2 h (69). Thyroid hormone increases fatty acid oxidation in an autophagy-dependent manner (70). However, their kinetics appear to be initially slower than that of lacritin, and none are transient. Transiently stimulated autophagy appears to be efficient and effective. It is possible that lacritin may stimulate autophagy in a pulsatile manner as tears are continually replenished on stressed eyes.

Stress appears to be a prerequisite for lacritin-stimulated autophagy. This principle is most clearly evident in cells co-expressing mutant huntingtin proteins Htt103Q (toxic and stressful) or Htt25Q (not toxic) with double labeled LC3. Were this not true, epithelia in contact with lacritin would be constitutively in an autophagy-stimulated state. Stress readies FOXO1 by acetylation (5). That ligation with ATG7 is dependent on lacritin suggests an "on switch" for lacritin-dependent autophagy. AKT phosphorylation of FOXO1 is a likely mechanism because lacritin activates AKT1 (v-akt murine thymoma viral oncogene homolog 1).[3] AKT is constitutively active in the

HCT116 colon cancer cells in which FOXO1-ATG7-stimulated autophagy was originally described (5).

By diverting damaged or aggregated proteins and organelles into autophagosomes, autophagy through proteolysis feeds cellular and mitochondrial metabolism (49). Lacritin-stimulated autophagy restored basal oxygen consumption and spare respiratory capacity to prestress levels within minutes. Eight minutes is the estimated half-life (71) for autophagosomes, and complete degradation and delipidation of autophagosomal LC3 require 30 min (42) with protein degradation first detectable within 10 min (72). Thus, degradation may be sufficient to restore oxidative phosphorylation in keeping with the abrogation of lacritin-stimulated mitochondrial fusion by shRNA knockdown of ATG7, although other more direct mechanisms are possible. Taken together, we describe lacritin as a novel regulator of homeostasis that rapidly diverts ubiquitinated proteins into the autophagosomal pathway and restores oxidative phosphorylation.

Acknowledgments—We thank James Casanova and Jing Yu for critically reading the manuscript and Beth Levine for suggestions. We also thank Jeffrey Romano for assistance analyzing blots. We gratefully acknowledge Ai Yamamoto (Columbia University) for pcDNA Htt25Q-mCFP and Htt103Q-mCFP, Jayanta Debnath (University of California at San Francisco) for pBABE-puro mCherry-EGFP-LC3B, Robert Weinberg (Whitehead Institute for Biomedical Research) for pBABE-hygro, and Elias Haddad (University of Montreal) for FOXO3Nt in pWPI and pWPI.

REFERENCES

1. Morimoto, R. I. (2008) Proteotoxic stress and inducible chaperone networks in neurodegenerative disease and aging. *Genes Dev.* **22,** 1427–1438
2. Levine, B., Mizushima, N., and Virgin, H. W. (2011) Autophagy in immunity and inflammation. *Nature* **469,** 323–335
3. Hotamisligil, G. S. (2006) Inflammation and metabolic disorders. *Nature* **444,** 860–867
4. Lamark, T., and Johansen, T. (2010) Autophagy: links with the proteasome. *Curr. Opin. Cell Biol.* **22,** 192–198
5. Zhao, Y., Yang, J., Liao, W., Liu, X., Zhang, H., Wang, S., Wang, D., Feng, J., Yu, L., and Zhu, W. G. (2010) Cytosolic FOXO1 is essential for the induction of autophagy and tumour suppressor activity. *Nat. Cell Biol.* **12,** 665–675
6. Warr, M. R., Binnewies, M., Flach, J., Reynaud, D., Garg, T., Malhotra, R., Debnath, J., and Passegué, E. (2013) FOXO3A directs a protective autophagy program in haematopoietic stem cells. *Nature* **494,** 323–327
7. Hu, M. C., Lee, D. F., Xia, W., Golfman, L. S., Ou-Yang, F., Yang, J. Y., Zou, Y., Bao, S., Hanada, N., Saso, H., Kobayashi, R., and Hung, M. C. (2004) IκB kinase promotes tumorigenesis through inhibition of forkhead FOXO3a. *Cell* **117,** 225–237
8. Shoji-Kawata, S., Sumpter, R., Leveno, M., Campbell, G. R., Zou, Z., Kinch, L., Wilkins, A. D., Sun, Q., Pallauf, K., MacDuff, D., Huerta, C., Virgin, H. W., Helms, J. B., Eerland, R., Tooze, S. A., Xavier, R., Lenschow, D. J., Yamamoto, A., King, D., Lichtarge, O., Grishin, N. V., Spector, S. A., Kaloyanova, D. V., and Levine, B. (2013) Identification of a candidate therapeutic autophagy-inducing peptide. *Nature* **494,** 201–206
9. Chen, L., Zhou, L., Chan, E. C., Neo, J., and Beuerman, R. W. (2011) Characterization of the human tear metabolome by LC-MS/MS. *J. Proteome Res.* **10,** 4876–4882
10. Herok, G. H., Mudgil, P., and Millar, T. J. (2009) The effect of Meibomian lipids and tear proteins on evaporation rate under controlled *in vitro* conditions. *Curr. Eye Res.* **34,** 589–597
11. Zhou, L., Beuerman, R. W., Chan, C. M., Zhao, S. Z., Li, X. R., Yang, H., Tong, L., Liu, S., Stern, M. E., and Tan, D. (2009) Identification of tear fluid biomarkers in dry eye syndrome using iTRAQ quantitative proteomics. *J. Proteome Res.* **8,** 4889–4905
12. Schaumberg, D. A., Sullivan, D. A., Buring, J. E., and Dana, M. R. (2003) Prevalence of dry eye syndrome among US women. *Am. J. Ophthalmol.* **136,** 318–326
13. Srinivasan, S., Thangavelu, M., Zhang, L., Green, K. B., and Nichols, K. K. (2012) iTRAQ quantitative proteomics in the analysis of tears in dry eye patients. *Invest. Ophthalmol. Vis. Sci.* **53,** 5052–5059
14. Nichols, J. J., and Green-Church, K. B. (2009) Mass spectrometry-based proteomic analyses in contact lens-related dry eye. *Cornea* **28,** 1109–1117
15. Green-Church, K. B., and Nichols, J. J. (2008) Mass spectrometry-based proteomic analyses of contact lens deposition. *Mol Vis.* **14,** 291–297
16. Koo, B. S., Lee, D. Y., Ha, H. S., Kim, J. C., and Kim, C. W. (2005) Comparative analysis of the tear protein expression in blepharitis patients using two-dimensional electrophoresis. *J. Proteome Res.* **4,** 719–724
17. Sanghi, S., Kumar, R., Lumsden, A., Dickinson, D., Klepeis, V., Trinkaus-Randall, V., Frierson, H. F., Jr., and Laurie, G. W. (2001) cDNA and genomic cloning of lacritin, a novel secretion enhancing factor from the human lacrimal gland. *J. Mol. Biol.* **310,** 127–139
18. Velez, V. F., Romano, J. A., McKown, R. L., Green, K., Zhang, L., Raab, R. W., Ryan, D. S., Hutnik, C. M., Frierson, H. F., Jr., and Laurie, G. W. (2013) Tissue transglutaminase is a negative regulator of monomeric lacritin bioactivity. *Invest. Ophthalmol. Vis. Sci.* **54,** 2123–2132
19. Schenk, S., Schoenhals, G. J., de Souza, G., and Mann, M. (2008) A high confidence, manually validated human blood plasma protein reference set. *BMC Med. Genomics* **1,** 41
20. Porter, D., Weremowicz, S., Chin, K., Seth, P., Keshaviah, A., Lahti-Domenici, J., Bae, Y. K., Monitto, C. L., Merlos-Suarez, A., Chan, J., Hulette, C. M., Richardson, A., Morton, C. C., Marks, J., Duyao, M., Hruban, R., Gabrielson, E., Gelman, R., and Polyak, K. (2003) A neural survival factor is a candidate oncogene in breast cancer. *Proc. Natl. Acad. Sci. U.S.A.* **100,** 10931–10936
21. Landgraf, P., Wahle, P., Pape, H. C., Gundelfinger, E. D., Kreutz, M. R. (2008) The survival-promoting peptide Y-P30 enhances binding of pleiotrophin to syndecan-2 and -3 and supports its neuritogenic activity. *J. Biol. Chem.* **283,** 25036–25045
22. Hosokawa, N., Sasaki, T., Iemura, S., Natsume, T., Hara, T., and Mizushima, N. (2009) Atg101, a novel mammalian autophagy protein interacting with Atg13. *Autophagy* **5,** 973–979
23. Mercer, C. A., Kaliappan, A., and Dennis, P. B. (2009) A novel, human Atg13 binding protein, Atg101, interacts with ULK1 and is essential for macroautophagy. *Autophagy* **5,** 649–662
24. Zhang, Y., Wang, N., Raab, R. W., McKown, R. L., Irwin, J. A., Kwon, I., van Kuppevelt, T. H., and Laurie, G. W. (2013) Targeting of heparanase-modified syndecan-1 by prosecretory mitogen lacritin requires conserved core GAGAL plus heparan and chondroitin sulfate as a novel hybrid binding site that enhances selectivity. *J. Biol. Chem.* **288,** 12090–12101
25. Ma, P., Beck, S. L., Raab, R. W., McKown, R. L., Coffman, G. L., Utani, A., Chirico, W. J., Rapraeger, A. C., and Laurie, G. W. (2006) Heparanase deglycanation of syndecan-1 is required for binding of the epithelial-restricted prosecretory mitogen lacritin. *J. Cell Biol.* **174,** 1097–1106
26. Wang, J., Wang, N., Xie, J., Walton, S. C., McKown, R. L., Raab, R. W., Ma, P., Beck, S. L., Coffman, G. L., Hussaini, I. M., and Laurie, G. W. (2006) Restricted epithelial proliferation by lacritin via PKCα-dependent NFAT and mTOR pathways. *J. Cell Biol.* **174,** 689–700
27. Seifert, K., Gandia, N. C., Wilburn, J. K., Bower, K. S., Sia, R. K., Ryan, D. S, Deaton, M. L., Still, K. M., Vassilev, V. C, Laurie, G. W., and McKown, R. L. (2012) Tear lacritin levels by age, sex, and time of day in healthy adults. *Invest. Ophthalmol. Vis. Sci.* **53,** 6610–6616
28. Pankiv, S., Clausen, T. H., Lamark, T., Brech, A., Bruun, J. A., Outzen, H., Øvervatn, A., Bjørkøy, G., and Johansen, T. (2007) p62/SQSTM1 binds directly to Atg8/LC3 to facilitate degradation of ubiquitinated protein aggregates by autophagy. *J. Biol. Chem.* **282,** 24131–24145
29. Filimonenko, M., Isakson, P., Finley, K. D., Anderson, M., Jeong, H., Melia, T. J., Bartlett, B. J., Myers, K. M., Birkeland, H. C., Lamark, T., Krainc, D., Brech, A., Stenmark, H., Simonsen, A., and Yamamoto, A. (2010) The selective macroautophagic degradation of aggregated proteins requires

the PI3P-binding protein Alfy. *Mol. Cell* **38,** 265–279
30. Lam, H., Bleiden, L., de Paiva, C. S., Farley, W., Stern, M. E., and Pflugfelder, S. C. (2009) Tear cytokine profiles in dysfunctional tear syndrome. *Am. J. Ophthalmol.* **147,** 198–205.e1
31. Barabino, S., Chen, Y., Chauhan, S., and Dana, R. (2012) Ocular surface immunity: homeostatic mechanisms and their disruption in dry eye disease. *Prog. Retin. Eye Res.* **31,** 271–285
32. Runge, S., Thøgersen, H., Madsen, K., Lau, J., and Rudolph, R. (2008) Crystal structure of the ligand-bound glucagon-like peptide-1 receptor extracellular domain. *J. Biol. Chem.* **283,** 11340–11347
33. Ma, P., Wang, N., McKown, R. L., Raab, R. W., and Laurie, G. W. (2008) Focus on molecules: lacritin. *Exp. Eye Res.* **86,** 457–458
34. McKown, R. L., Wang, N., Raab, R. W., Karnati, R., Zhang, Y., Williams, P. B., and Laurie, G. W. (2009) Lacritin and other new proteins of the lacrimal functional unit. *Exp. Eye Res.* **88,** 848–858
35. Lohmander, L. S., Hascall, V. C., and Caplan, A. I. (1979) Effects of 4-methyl umbelliferyl-β-D-xylopyranoside on chondrogenesis and proteoglycan synthesis in chick limb bud mesenchymal cell cultures. *J. Biol. Chem.* **254,** 10551–10561
36. Kakizaki, I., Kojima, K., Takagaki, K., Endo, M., Kannagi, R., Ito, M., Maruo, Y., Sato, H., Yasuda, T., Mita, S., Kimata, K., and Itano, N. (2004) A novel mechanism for the inhibition of hyaluronan biosynthesis by 4-methylumbelliferone. *J. Biol. Chem.* **279,** 33281–33289
37. Lipinski, M. M., Hoffman, G., Ng, A., Zhou, W., Py, B. F., Hsu, E., Liu, X., Eisenberg, J., Liu, J., Blenis, J., Xavier, R. J., and Yuan, J. (2010) A genome-wide siRNA screen reveals multiple mTORC1 independent signaling pathways regulating autophagy under normal nutritional conditions. *Dev. Cell* **18,** 1041–1052
38. Ravikumar, B., Vacher, C., Berger, Z., Davies, J. E., Luo, S., Oroz, L. G., Scaravilli, F., Easton, D. F., Duden, R., O'Kane, C. J., and Rubinsztein, D. C. (2004) Inhibition of mTOR induces autophagy and reduces toxicity of polyglutamine expansions in fly and mouse models of Huntington disease. *Nat. Genet.* **36,** 585–595
39. Grzelkowska-Kowalczyk, K., and Wieteska-Skrzeczyńska, W. (2010) Treatment with TNF-alpha and IFN-gamma alters the activation of SER/THR protein kinases and the metabolic response to IGF-I in mouse c2c12 myogenic cells. *Cell. Mol. Biol. Lett.* **15,** 13–31
40. Høyer-Hansen, M., Bastholm, L., Szyniarowski, P., Campanella, M., Szabadkai, G., Farkas, T., Bianchi, K., Fehrenbacher, N., Elling, F., Rizzuto, R., Mathiasen, I. S., and Jäättelä, M. (2007) Control of macroautophagy by calcium, calmodulin-dependent kinase kinase-β, and Bcl-2. *Mol. Cell.* **25,** 193–205
41. Lara-Pezzi, E., Winn, N., Paul, A., McCullagh, K., Slominsky, E., Santini, M. P., Mourkioti, F., Sarathchandra, P., Fukushima, S., Suzuki, K., and Rosenthal, N. (2007) A naturally occurring calcineurin variant inhibits FoxO activity and enhances skeletal muscle regeneration. *J. Cell Biol.* **179,** 1205–1218
42. Tanida, I., Sou, Y. S., Ezaki, J., Minematsu-Ikeguchi, N., Ueno, T., and Kominami, E. (2004) HsAtg4B/HsApg4B/autophagin-1 cleaves the carboxyl termini of three human Atg8 homologues and delipidates microtubule-associated protein light chain 3- and $GABA_A$ receptor-associated protein-phospholipid conjugates. *J. Biol. Chem.* **279,** 36268–36276
43. Yamamoto, A., Cremona, M. L., and Rothman, J. E. (2006) Autophagy-mediated clearance of huntingtin aggregates triggered by the insulin-signaling pathway. *J. Cell Biol.* **172,** 719–731
44. Ciani, B., Layfield, R., Cavey, J. R., Sheppard, P. W., and Searle, M. S. (2003) Structure of the ubiquitin-associated domain of p62 (SQSTM1) and implications for mutations that cause Paget's disease of bone. *J. Biol. Chem.* **278,** 37409–37412
45. Yoon, K., Jung, E. J., Lee, S. R., Kim, J., Choi, Y., and Lee, S. Y. (2008) TRAF6 deficiency promotes TNF-induced cell death through inactivation of GSK3beta. *Cell Death Differ.* **15,** 730–738
46. Xia, Z. P., Sun, L., Chen, X., Pineda, G., Jiang, X., Adhikari, A., Zeng, W., and Chen, Z. J. (2009) Direct activation of protein kinases by unanchored polyubiquitin chains. *Nature* **461,** 114–119
47. Matsumoto, G., Wada, K., Okuno, M., Kurosawa, M., and Nukina, N. (2011) Serine 403 phosphorylation of p62/SQSTM1 regulates selective autophagic clearance of ubiquitinated proteins. *Mol. Cell* **44,** 279–289
48. Wu, J. J., Quijano, C., Chen, E., Liu, H., Cao, L., Fergusson, M. M., Rovira, I. I., Gutkind, S., Daniels, M. P., Komatsu, M., and Finkel, T. (2009) Mitochondrial dysfunction and oxidative stress mediate the physiological impairment induced by the disruption of autophagy. *Aging* **1,** 425–437
49. Guo, J. Y., Chen, H. Y., Mathew, R., Fan, J., Strohecker, A. M., Karsli-Uzunbas, G., Kamphorst, J. J., Chen, G., Lemons, J. M., Karantza, V., Coller, H. A., Dipaola, R. S., Gelinas, C., Rabinowitz, J. D., and White, E. (2011) Activated Ras requires autophagy to maintain oxidative metabolism and tumorigenesis. *Genes Dev.* **25,** 460–470
50. van der Windt, G. J., Everts, B., Chang, C. H., Curtis, J. D., Freitas, T. C., Amiel, E., Pearce, E. J., and Pearce, E. L. (2012) Mitochondrial respiratory capacity is a critical regulator of $CD8^+$ T cell memory development. *Immunity* **36,** 68–78
51. Youle, R. J., and van der Bliek, A. M. (2012) Mitochondrial fission, fusion, and stress. *Science* **337,** 1062–1065
52. Sauer, L. A., Dauchy, R. T., Nagel, W. O., and Morris, H. P. (1980) Mitochondrial malic enzymes. Mitochondrial $NAD(P)^+$-dependent malic enzyme activity and malate-dependent pyruvate formation are progression-linked in Morris hepatomas. *J. Biol. Chem.* **255,** 3844–3848
53. Campesan, S., Green, E. W., Breda, C., Sathyasaikumar, K. V., Muchowski, P. J., Schwarcz, R., Kyriacou, C. P., and Giorgini, F. (2011) The kynurenine pathway modulates neurodegeneration in a *Drosophila* model of Huntington's disease. *Curr. Biol.* **21,** 961–966
54. Bitterman, K. J., Anderson, R. M., Cohen, H. Y., Latorre-Esteves, M., and Sinclair, D. A. (2002) Inhibition of silencing and accelerated aging by nicotinamide, a putative negative regulator of yeast sir2 and human SIRT1. *J. Biol. Chem.* **277,** 45099–45107
55. Riggs, T. R., and Hegsted, D. M. (1948) The effect of pantothenic acid deficiency on acetylation in rats. *J. Biol. Chem.* **172,** 539–545
56. Eisenberg, T., Knauer, H., Schauer, A., Büttner, S., Ruckenstuhl, C., Carmona-Gutierrez, D., Ring, J., Schroeder, S., Magnes, C., Antonacci, L., Fussi, H., Deszcz, L., Hartl, R., Schraml, E., Criollo, A., Megalou, E., Weiskopf, D., Laun, P., Heeren, G., Breitenbach, M., Grubeck-Loebenstein, B., Herker, E., Fahrenkrog, B., Fröhlich, K. U., Sinner, F., Tavernarakis, N., Minois, N., Kroemer, G., and Madeo, F. (2009) Induction of autophagy by spermidine promotes longevity. *Nat. Cell Biol.* **11,** 1305–1314
57. Wu, Z., Lauer, T. W., Sick, A., Hackett, S. F., and Campochiaro, P. A. (2007) Oxidative stress modulates complement factor H expression in retinal pigmented epithelial cells by acetylation of FOXO3. *J. Biol. Chem.* **282,** 22414–22425
58. Behrends, C., Sowa, M. E., Gygi, S. P., and Harper, J. W. (2010) Network organization of the human autophagy system. *Nature* **466,** 68–76
59. van Grevenynghe, J., Procopio, F. A., He, Z., Chomont, N., Riou, C., Zhang, Y., Gimmig, S., Boucher, G., Wilkinson, P., Shi, Y., Yassine-Diab, B., Said, E. A., Trautmann, L., El Far, M., Balderas, R. S., Boulassel, M. R., Routy, J. P., Haddad, E. K., and Sekaly, R. P. (2008) Transcription factor FOXO3a controls the persistence of memory $CD4^+$ T cells during HIV infection. *Nat. Med.* **14,** 266–274
60. Laurie, G. W., Olsakovsky, L. A., Conway, B. P., McKown, R. L., Kitagawa, K., and Nichols, J. J. (2008) Dry eye and designer ophthalmics. *Optom. Vis. Sci.* **85,** 643–652
61. Zheng, X., De Paiva, C. S., Rao, K., Li, D. Q., Farley, W. J., Stern, M., and Pflugfelder, S. C. (2010) Evaluation of the transforming growth factor-β activity in normal and dry eye human tears by CCL-185 cell bioassay. *Cornea* **29,** 1048–1054
62. Qi, H., Shine, H. D., Li, D. Q., de Paiva, C. S., Farley, W. J., Jones, D. B., and Pflugfelder S. C. (2008) Glial cell-derived neurotrophic factor gene delivery enhances survival of human corneal epithelium in culture and the overexpression of GDNF in bioengineered constructs. *Exp. Eye Res.* **87,** 580–586
63. Kakazu, A., Chandrasekher, G., and Bazan HE. (2004) HGF protects corneal epithelial cells from apoptosis by the PI-3K/Akt-1/Bad- but not the ERK1/2-mediated signaling pathway. *Invest. Ophthalmol. Vis. Sci.* **45,** 3485–3492
64. Ozyildirim, A. M., Wistow, G. J., Gao, J., Wang, J., Dickinson, D. P., Frierson, H. F., Jr., and Laurie, G. W. (2005) The lacrimal gland transcriptome is an unusually rich source of rare and poorly characterized gene transcripts. *Invest. Ophthalmol. Vis. Sci.* **46,** 1572–1580

65. Fleiszig, S. M., Kwong, M. S., and Evans, D. J. (2003) Modification of *Pseudomonas aeruginosa* interactions with corneal epithelial cells by human tear fluid. *Infect. Immun.* **71,** 3866–3874
66. Malik, S. A., Mariño, G., BenYounès, A., Shen, S., Harper, F., Maiuri, M. C., and Kroemer, G. (2011) Neuroendocrine regulation of autophagy by leptin. *Cell Cycle* **10,** 2917–2923
67. Seibenhener, M. L., Babu, J. R., Geetha, T., Wong, H. C., Krishna, N. R., and Wooten MW. (2004) Sequestosome 1/p62 is a polyubiquitin chain binding protein involved in ubiquitin proteasome degradation. *Mol. Cell Biol.* **24,** 8055–8068
68. Duran, A., Amanchy, R., Linares, J. F., Joshi, J., Abu-Baker, S., Porollo, A., Hansen, M., Moscat, J., and Diaz-Meco, M. T. (2011) p62 is a key regulator of nutrient sensing in the mTORC1 pathway. *Mol. Cell* **44,** 134–146
69. Pilli, M., Arko-Mensah, J., Ponpuak, M., Roberts, E., Master, S., Mandell, M. A., Dupont, N., Ornatowski, W., Jiang, S., Bradfute, S. B., Bruun, J. A., Hansen, T. E., Johansen, T., and Deretic, V. (2012) TBK-1 promotes autophagy-mediated antimicrobial defense by controlling autophagosome maturation. *Immunity* **37,** 223–234
70. Sinha, R. A., You, S. H., Zhou, J., Siddique, M. M., Bay, B. H., Zhu, X., Privalsky, M. L., Cheng, S. Y., Stevens, R. D., Summers, S. A., Newgard, C. B., Lazar, M. A., and Yen, P. M. (2012) Thyroid hormone stimulates hepatic lipid catabolism via activation of autophagy. *J. Clin. Investig.* **122,** 2428–2438
71. Yoshimori, T. (2004) Autophagy: a regulated bulk degradation process inside cells. *Biochem. Biophys. Res. Commun.* **313,** 453–458
72. Seglen, P. O., and Gordon, P. B. (1982) 3-Methyladenine: specific inhibitor of autophagic/lysosomal protein degradation in isolated rat hepatocytes. *Proc. Natl. Acad. Sci. U.S.A.* **79,** 1889–1892